Statically Determinate Curved Members 6

Abstract

Chapter 3 dealt with beams, which are *straight* members subjected to transverse loading. We showed there that transversely loaded beams respond by bending, i.e., they equilibrate the loading by developing internal shear and moment quantities. When the centroidal axis is curved, the behavior of a curved member subjected to transverse loading can undergo a dramatic change from predominately bending action to predominately axial action depending on how the ends are restrained. This characteristic of curved members makes them more efficient than straight members for spanning moderate to large scale openings. A typical application is an arch structure, which is composed of curved members restrained at their ends.

In this chapter, we first develop the general solution for the internal forces existing in a planar curved member and apply it to members having parabolic and circular shapes. Next, we introduce the method of virtual forces specialized for planar curved members and illustrate its application to compute displacements for various geometries. The last section of the chapter deals with the optimal shape for an arch and the analysis of three-hinged arches, a popular form of arch structure. The material presented here also provides the basis for the analysis of statically indeterminate arches treated in Chap. 9.

6.1 A Brief History of Arch-Type Structures

We define an arch as a curved member that spans an opening and is restrained against movement at its ends by abutments. Figure 6.1 illustrates this definition. Arches are designed to carry a vertical loading which, because of the curved nature of the member, is partially resisted by horizontal forces

J.J. Connor, S. Faraji, *Fundamentals of Structural Engineering*,
DOI 10.1007/978-3-319-24331-3_6

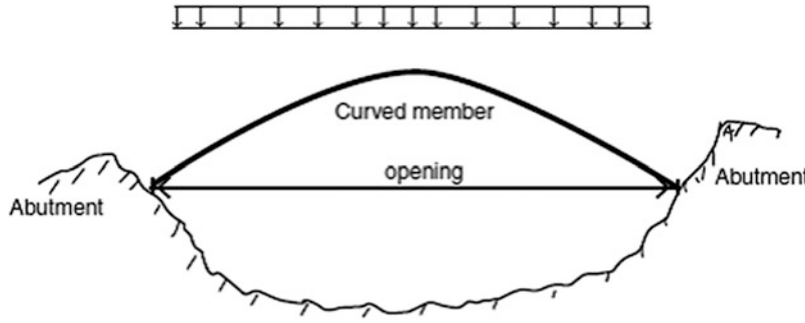

Fig. 6.1 Definition of an arch

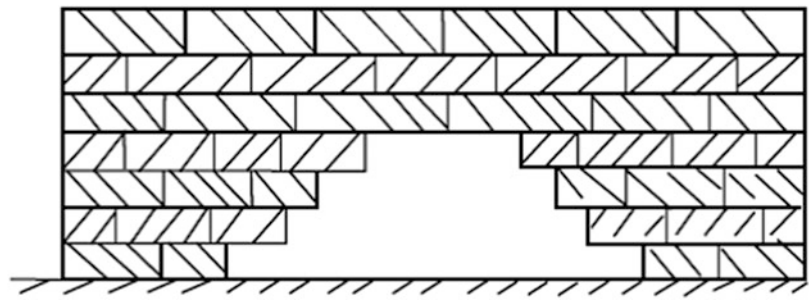

Fig. 6.2 Corbel arch

provided by the abutments. Arches generally are more efficient than straight beam-type structures for spanning an opening since their geometry can be modified so that they carry the transverse loading almost completely by axial action, i.e., by compression. However, abutments are required to develop the compression-type behavior, and this requirement sometimes limits the applicability of the arch for a particular site.

In what follows, we briefly discuss the historical development of arch structures and then present the underlying theory for statically determinate curved members. This theory is similar to the theory for gable roof structures presented in Chap. 4. Later, in Chap. 9, we discuss the theory of statically indeterminate curved members.

Arches have many applications. They are used for openings in walls, for crossing gorges and rivers, and as monumental structures such as the Arc de Triomphe. The first application of arch-type construction in buildings occurred around 4000 BC in Egypt and Greece. Openings in walls were spanned using the scheme shown in Fig. 6.2. Large flat stones were stacked in layers of increasing width until they met at the top layer. Each layer was stabilized by the weight applied above the layer. The concept is called a Corbel arch. No formwork is required to construct the structure. Also, no horizontal thrust and therefore no abutments are needed. The term "false arch" is sometimes used to describe this type of structure. False arches were used almost exclusively in ancient Greece where the techniques of masonry construction were perfected.

The type of arch construction shown in Fig. 6.3 for carrying vertical loading across an opening was introduced by the Egyptians around 3000 BC. It employs tapered stones, called voussoirs, which are arranged around a curved opening in such a manner that each brick is restrained by compressive and frictional forces. The system is unstable until the last stone, called the "keystone," is placed. Consequently, temporary framework is required during construction.

Starting around 300 BC, the Romans perfected masonry arch construction and built some unique structures, many of which are still functioning after 2000 years. They preferred circular arches and

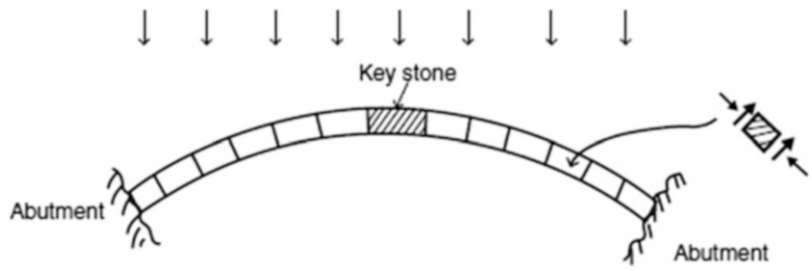

Fig. 6.3 Keystone arch construction

Fig. 6.4 Pont du Gard crossing

included them in buildings, bridges, and aqueducts. One of the most famous examples is the Pont du Gard, shown in Fig. 6.4; a bridge/aqueduct over the river Gard built in 19 BC. Some of the stones weigh up to 6 ton.

Another example of a second-century multiple span Roman arch masonry bridge is shown in Fig. 6.5. The typical span length is 98 ft. This bridge crosses the Tagus River in Spain and was a key element in the transportation network connecting the outer Roman Provinces with Rome.

Masonry materials are ideal for arch construction since they are strong under compression and also very durable. However, it is difficult to construct long span masonry arch bridges. With the development of alternate structural materials such as cast iron and steel at the end of the eighteenth century, there was a shift toward arches formed with metal members. Figure 6.6 shows the Iron Bridge built in 1781. The main span is 100 ft and crosses the Severn Gorge in the UK. Each of the members was formed using cast iron technology which was evolving at the time. Since cast iron is weak in tension and tends to fail in a brittle manner, it was shortly replaced as the material of choice by steel.

The development of railroads created a demand for bridges with more load capacity and longer spans. During this time period, there were many arch bridges constructed. Figure 6.7 shows the Eads Bridge built in 1874 across the Mississippi River in St. Louis, Missouri. This bridge has ribbed steel arch spans of 520 ft, fabricated with tubular structural alloy steel members; the first use of steel in a

Fig. 6.5 Alcantara Toledo bridge

Fig. 6.6 Iron Bridge, England

major bridge project. Today, the bridge is still carrying pedestrian, vehicular, and light rail traffic across the Mississippi.

At the end of the nineteenth century, reinforced concrete emerged as a major competitor to steel as a structural material. Reinforced concrete allowed one to form arch geometries that were aesthetically more pleasing than conventional steel arch geometries, and therefore became the preferred material. Most of this surge in popularity was due to the work of Robert Maillart, a Swiss Engineer

Fig. 6.7 Eads Bridge, USA

Fig. 6.8 Salginatobel Bridge, Switzerland

(1872–1940), who developed arch concepts that revolutionized the design practice for reinforced concrete arches. An example is the Salginatobel Bridge, shown in Fig. 6.8. This bridge, built in 1930, crosses the Salgina Valley Ravine in Switzerland with a span of 270 ft. It is the ideal solution for this picturesque site and has been recognized by ASCE as a landmark project.

A unique arch bridge in the USA is the New Gorge Steel Arch Bridge located in West Virginia. Opened in 1977, it has the longest main span (1700 ft) and highest height (876 ft) of all arch bridges in North and South America. It held the world record for span and height until 2003 when the Lupu Arch Bridge in Shanghai (1800 ft span) was opened. A type of weathering steel called Corten was used in the New Gorge Arch structure in order to avoid the need for periodic painting.

Another unique arch bridge in the USA is the Hoover Dam Bypass Bridge. Segmented concrete construction was used to fabricate the concrete box elements in situ. The construction process employed a complex tieback scheme, as illustrated in Fig. 6.9b–d. The bridge was completed in 2010.

Fig. 6.9 Modern Arch Bridges in the USA. (**a**) New Gorge Arch, West Virginia. (**b**) Hoover Dam Bypass—under construction. (**c**) Hoover Dam Bypass—under construction. (**d**) Hoover Dam Bypass—under construction. (**e**) Hoover Dam Bypass—completed

6.2 Modeling of Arch Structures

We idealize an arch structure as a curved member restrained at its ends with a combination of fixed, hinged, and roller supports. Figure 6.10 illustrates various types of end conditions. Case (a) corresponds to full end fixity, a condition that is difficult to achieve. The more common case is (b) where the abutments can prevent translation but not rotation. We refer to this structure as a two-hinged arch. The third case, (c), corresponds to a "tied arch structure" where the ends are interconnected with a tension member. This scheme is used when the abutments are not capable of resisting the horizontal thrust action of the arch.

If the arch is a bridge, the roadway may be connected above the structure as in Fig. 6.11a, or below the structure as in Fig. 6.11b. When placed above, the deck weight is transmitted by compression members to the arch. Decks placed below the arch are supported by cables. Both loading cases are idealized as a uniform loading *per horizontal projection* as shown in Fig. 6.11c. In some cases, soil backfill is placed between the roadway and the arch. The soil loading is represented as a nonuniform loading whose shape is defined by the arch geometry. Figures 6.11d, e illustrate this case.

The structures in Fig. 6.10 are statically indeterminate. We can reduce the two-hinge arch to a statically determinate structure by converting it to a three-hinge arch. The additional hinge is usually placed at mid-span as shown in Fig. 6.12.

In this chapter, we first present a general theory of statically determinate curved members and then specialize the general theory for three-hinge arches. We treat statically indeterminate arches later in Chap. 9.

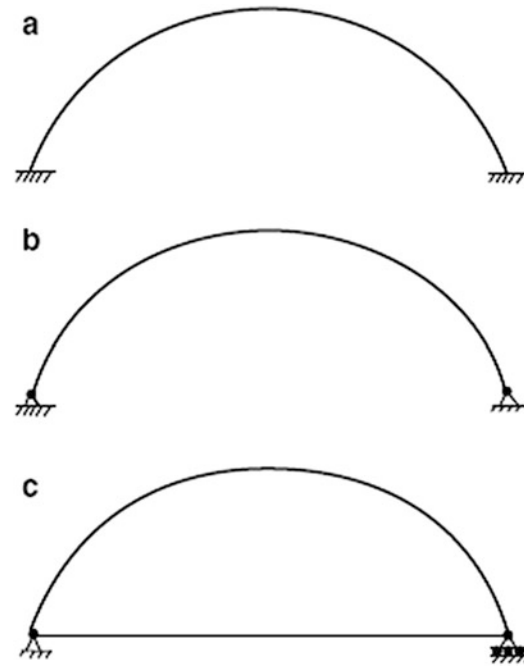

Fig. 6.10 Indeterminate Arch structures with various end fixity conditions. (**a**) Fully fixed Arch—3° indeterminate. (**b**) Two-hinged arch—1° indeterminate. (**c**) Tied arch—1° indeterminate

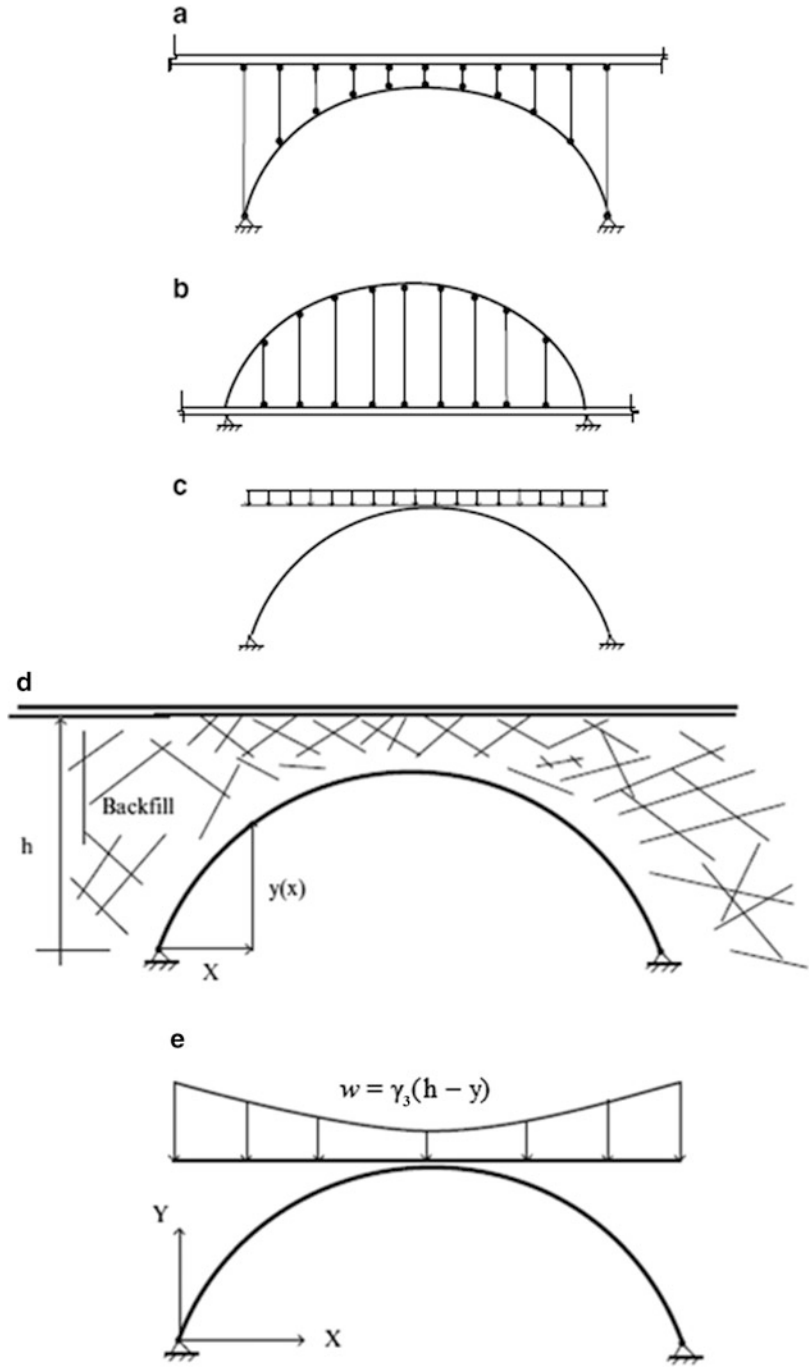

Fig. 6.11 Different roadway arrangements—idealized loading. (**a**) Roadway above the arch. (**b**) Roadway below the arch. (**c**) Idealized uniform dead loading. (**d**) Soil backfill above the arch. (**e**) Idealized soil loading

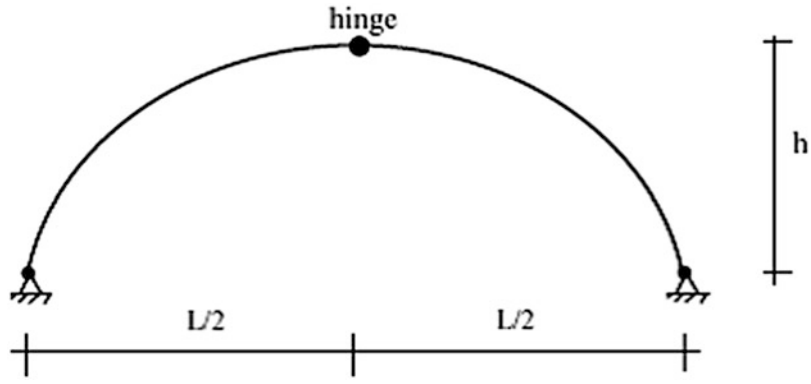

Fig. 6.12 Three-hinge arch

6.3 Internal Forces in Curved Members

We consider the statically determinate curved member shown in Fig. 6.13a. We work with a Cartesian reference frame having axes X and Y and define the centroidal axis of the member by the function, $y = y(x)$. The vertical loading is assumed to be expressed in terms of the horizontal projected length. These choices are appropriate for the arch structures described in the previous section. We determine the reactions using the global equilibrium equations.

The applied load is equilibrated by internal forces, similar to the behavior of a straight beam under transverse load. To determine these internal forces, we isolate an arbitrary segment such as AC defined in Fig. 6.13b. We work initially with the internal forces referred to the $X - Y$ frame and then transform them over to the local tangential/normal frame. Note that now there may be a longitudinal force component as well as a transverse force component, whereas straight beams subjected to transverse loading have no longitudinal component.

Enforcing equilibrium leads to the general solution for the internal forces.

$$\begin{aligned} F_x &= -R_{\mathrm{A}x} \\ F_y &= -R_{\mathrm{A}y} + \int_0^x w(x)\mathrm{d}\xi \\ M &= xR_{\mathrm{A}y} - yR_{\mathrm{A}x} - \int_0^x w(x)\xi\,\mathrm{d}\xi \end{aligned} \tag{6.1}$$

Lastly, we transform the Cartesian force components (F_x, F_y) over to the tangential/normal frame (F, V). Noting Fig. 6.14, the transformation law is

$$\begin{aligned} F &= F_y \sin\theta + F_x \cos\theta \\ V &= F_y \cos\theta - F_x \sin\theta \\ \tan\theta &= \frac{\mathrm{d}y}{\mathrm{d}x} \end{aligned} \tag{6.2}$$

In order to evaluate the axial (F) and shear forces (V), we need to specify the angle θ between the tangent and the horizontal axis. This quantity depends on $y(x)$, the function that defines the shape of the centroidal axis.

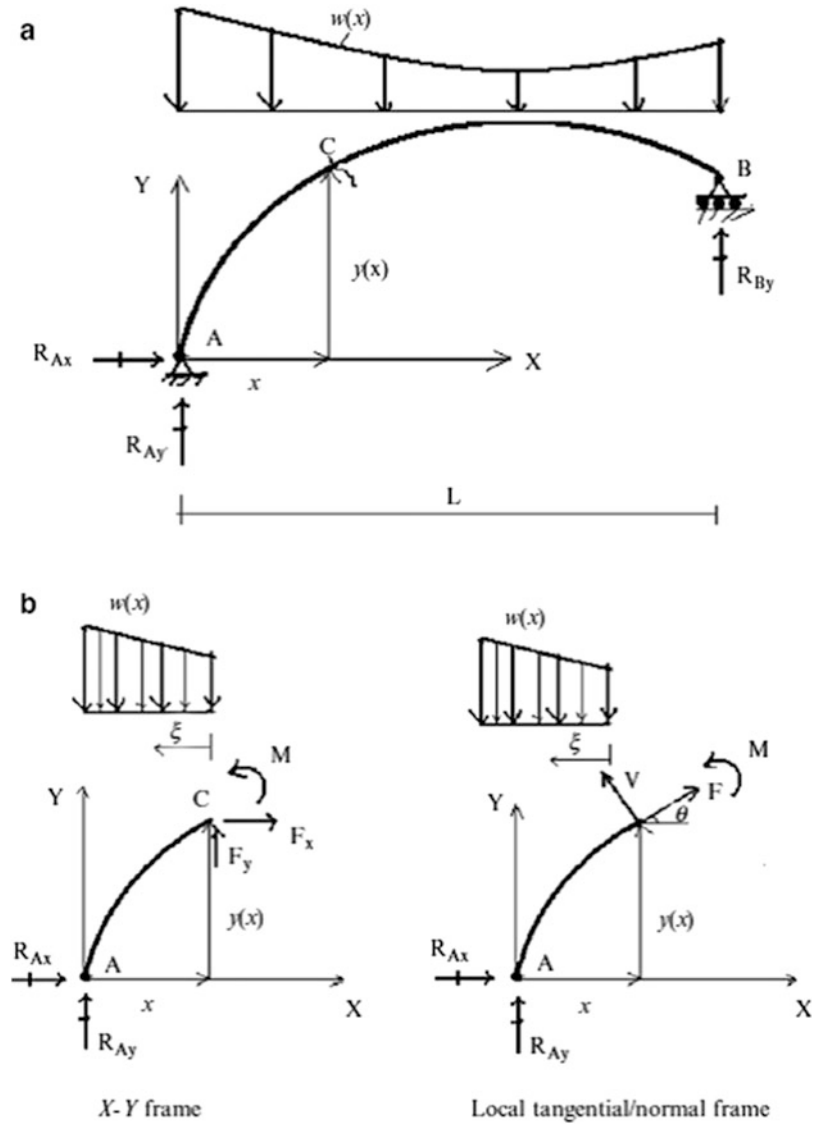

Fig. 6.13 (**a**) Notation for statically determinate curved member. (**b**) Free body diagram—curved beam. $X - Y$ frame. Local tangential/normal frame

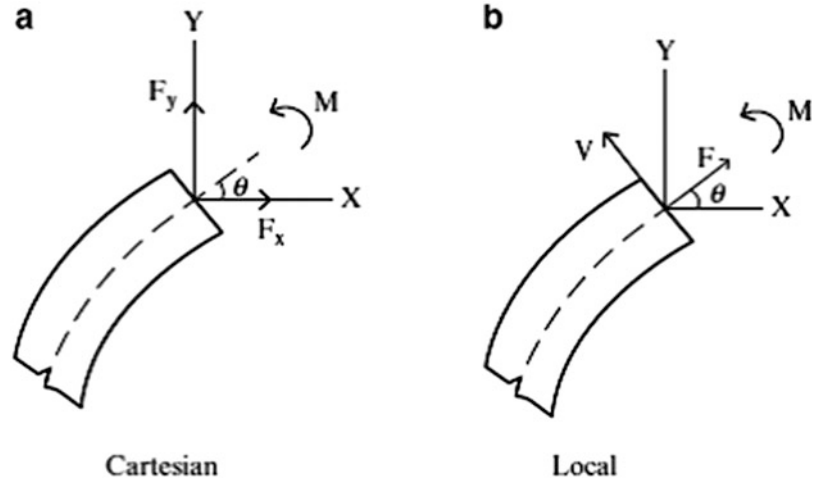

Fig. 6.14 Cartesian—local force components

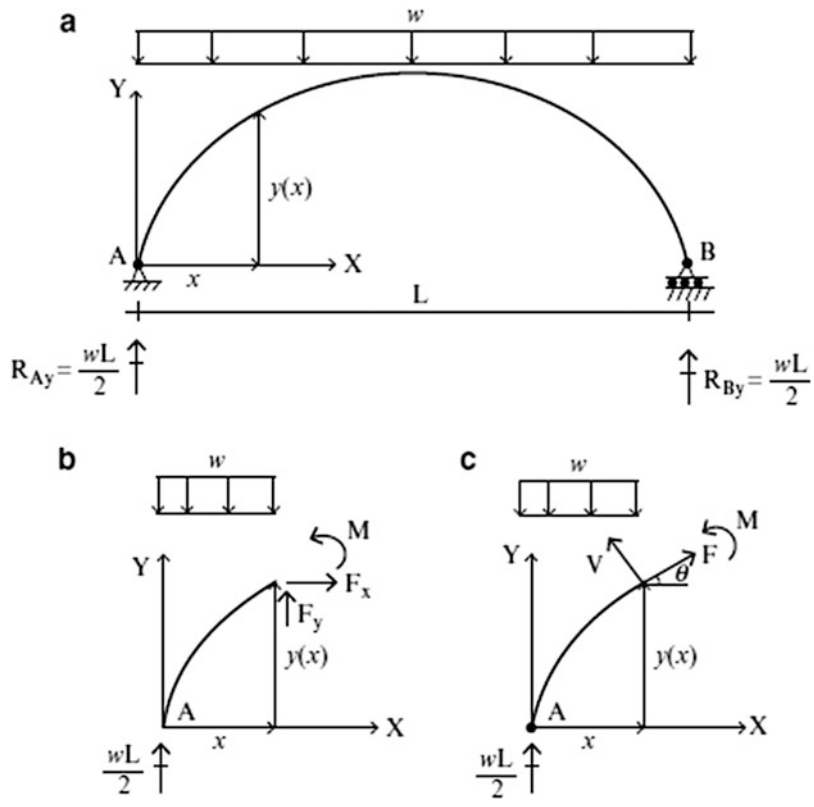

Fig. 6.15 Curved member—uniform vertical loading. (**a**) Reactions. (**b**) Internal forces—Cartesian frame. (**c**) Internal forces—local frame

We specialize the above set of equations for a symmetrical curved member where the loading consists of

(a) A uniform vertical loading per projected length defined in Fig. 6.15.
(b) A concentrated load at the crown defined in Fig. 6.16.

(a) *Uniformly distributed load* (Fig. 6.15):
Enforcing equilibrium and symmetry leads to

$$R_{Ax} = 0 \quad R_{Ay} = R_{By} = \frac{wL}{2}$$
$$F_x = 0 \quad F_y = -\frac{wL}{2} + wx$$
$$M = \frac{wL}{2}x - \frac{wx^2}{2}$$

Note that these results are the *same* as for a simply supported straight beam subjected to transverse loading. Substituting for F_x and F_y in (6.2) results in the internal forces (F, V, M) due to a uniform vertical loading,

$$F = \left(-\frac{wL}{2} + wx\right)\sin\theta$$
$$V = \left(-\frac{wL}{2} + wx\right)\cos\theta \tag{6.3}$$
$$M = \frac{wL}{2}x - \frac{wx^2}{2}$$

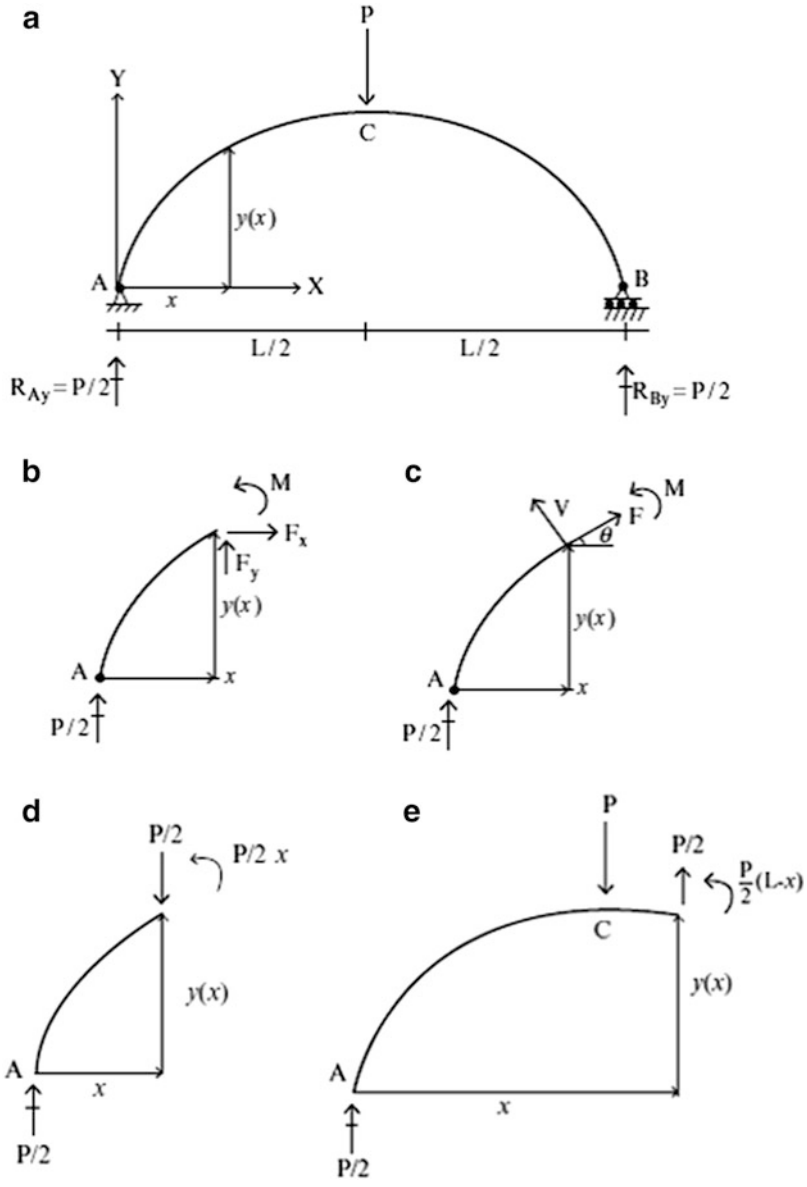

Fig. 6.16 Curved member—concentrated load. (**a**) Reactions. (**b**) Internal forces—Cartesian frame. (**c**) Internal forces—local frame. (**d**) Segment AC $0 \leq x < L/2$. (**e**) Segment CB $L/2 < x \leq L$

(b) *Concentrated load* (Fig. 6.16):
The internal forces referred to the Cartesian frame are

Segment AC $0 \leq x < L/2$	Segment CB $L/2 < x \leq L$
$F_x = 0$	$F_x = 0$
$F_y = -\frac{P}{2}$	$F_y = \frac{P}{2}$
$M = \frac{P}{2}x$	$M = \frac{P}{2}(L - x)$

Substituting for F_x and F_y in (6.2) results in the internal forces (F, V, M) in the local frame,

$$\begin{array}{ll} \text{For} \quad 0 \le x < L/2 & \text{For} \quad L/2 < x \le L \\ F = -\dfrac{P}{2}\sin\theta & F = +\dfrac{P}{2}\sin\theta \\ V = -\dfrac{P}{2}\cos\theta & V = +\dfrac{P}{2}\cos\theta \\ M = \dfrac{P}{2}x & M = \dfrac{P}{2}(L-x) \end{array} \tag{6.4}$$

6.4 Parabolic Geometry

We will show later that a parabolic arch is the optimal shape for a uniform vertical loading, in the sense that there is essentially no bending, only axial force, introduced by this loading. Using the notation defined in Fig. 6.17, the parabolic curve is expressed in terms of h, the height at mid-span, and the dimensionless coordinate, x/L.

$$y(x) = 4h\left[\frac{x}{L} - \left(\frac{x}{L}\right)^2\right] \tag{6.5}$$

Differentiating $y(x)$ leads to

$$\tan\theta = \frac{\mathrm{d}y}{\mathrm{d}x} = 4\frac{h}{L}\left(1 - 2\frac{x}{L}\right) \tag{6.6}$$

The maximum value of θ is at $x = 0, L$

$$\theta_{\max} = \pm\tan^{-1}\left(4\frac{h}{L}\right)$$

Values of $\theta_{\max}$ vs. h/L are tabulated in the table below.

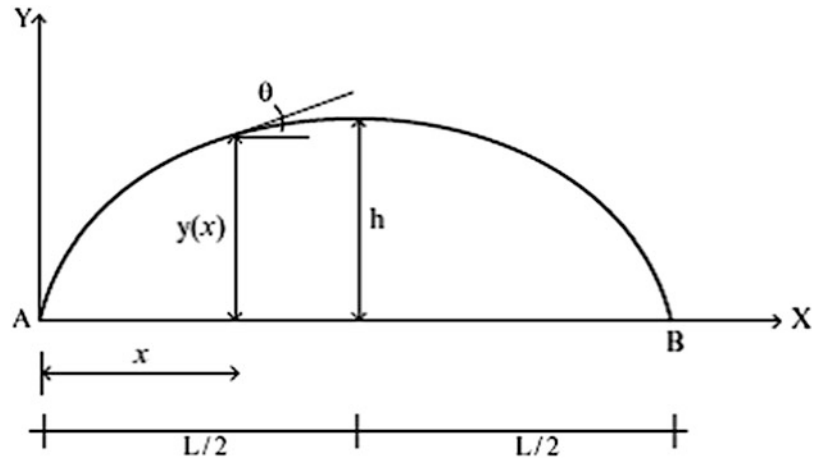

Fig. 6.17 Notation for parabolic shape function

$\frac{h}{L}$	$\theta_{max}(^\circ)$	$\tan\theta_{max}$	$\cos\theta_{max}$	$\sin\theta_{max}$
0	0	0	1	0
0.01	2.3	0.04	0.999	0.04
0.025	5.7	0.1	0.995	0.099
0.05	11.3	0.2	0.98	0.196
0.1	21.8	0.4	0.93	0.37
0.15	30.9	0.6	0.86	0.51
0.2	38.6	0.8	0.78	0.62
0.25	45	1	0.7	0.7
0.3	50.2	1.2	0.64	0.77
0.35	54.4	1.4	0.58	81
0.4	58	1.6	0.53	0.85
0.45	60.9	1.8	0.48	0.87
0.5	63.4	2	0.45	0.89

The parameter h/L is a measure of the steepness of the curved member. Deep curved members have $h/L \geq \approx 0.25$. A curved member is said to be shallow when h/L is small with respect to unity, on the order of 0.1. The trigonometric measures for a shallow curved member are approximated by

$$\text{shallow parabolic curve} \begin{cases} \tan\theta = \dfrac{dy}{dx} \approx \theta(\text{rad}) \\ \cos\theta = \dfrac{1}{\sqrt{1+\tan\theta^2}} \approx 1 \\ \sin\theta = \dfrac{\tan\theta}{\sqrt{1+\tan\theta^2}} \approx \tan\theta \approx \theta(\text{rad}) \end{cases} \tag{6.7}$$

Example 6.1 Shallow vs. Deep Parabolic Curved Members

Given: The parabolic curved beam defined in Fig. E6.1a.

Determine: The axial, shear, and moment distributions for (a) $h/L = 0.1$, (b) $h/L = 0.5$.

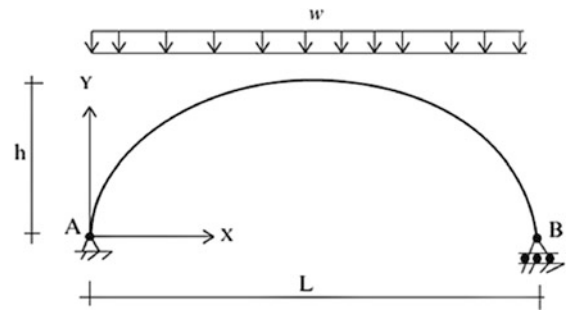

Fig. E6.1a Parabolic geometry

Solution: Enforcing equilibrium and symmetry leads to the reactions listed in Fig. E6.1b.

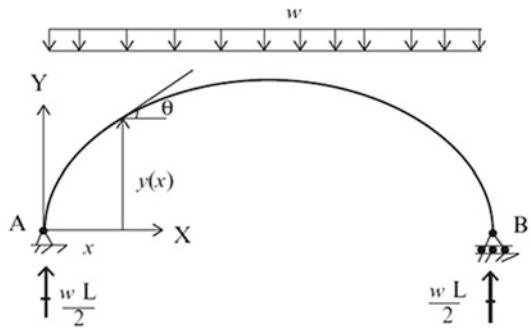

Fig. E6.1b Reactions

Applying (6.3) and (6.5), the internal forces in the local frame are

$$F = \left(-\frac{wL}{2} + wx\right)\sin\theta$$
$$V = \left(-\frac{wL}{2} + wx\right)\cos\theta$$
$$M = \frac{wL}{2}x - \frac{wx^2}{2}$$

where

$$\cos\theta = \frac{1}{\sqrt{1 + \left(4\frac{h}{L}\left(1 - 2\frac{x}{L}\right)\right)^2}}$$
$$\sin\theta = \frac{4\frac{h}{L}\left(1 - 2\frac{x}{L}\right)}{\sqrt{1 + \left(4\frac{h}{L}\left(1 - 2\frac{x}{L}\right)\right)^2}}$$

The internal forces are listed in the table below and plotted in Figs. E6.1c, E6.1d, and E6.1e for $h/L = 0.1$ and $h/L = 0.5$. Note that the moment is independent of h/L.

		$\frac{h}{L} = 0.1$		$\frac{h}{L} = 0.5$	
$\frac{x}{L}$	$\frac{M}{wL^2}$	$\frac{V}{wL}$	$\frac{F}{wL}$	$\frac{V}{wL}$	$\frac{F}{wL}$
0	0	−0.464	−0.186	−0.224	−0.447
0.1	0.045	−0.381	−0.122	−0.212	−0.339
0.2	0.08	−0.292	−0.07	−0.192	−0.125
0.3	0.105	−0.197	−0.032	−0.156	−0.125
0.4	0.12	−0.1	−0.008	−0.093	−0.037
0.5	0.125	0	0	0	0
0.6	0.12	0.1	−0.008	0.093	−0.037
0.7	0.105	0.197	−0.032	0.156	−0.125
0.8	0.08	0.292	−0.07	0.192	−0.23
0.9	0.045	0.381	−0.122	0.212	−0.339

$\frac{x}{L}$	$\frac{M}{wL^2}$	$\frac{h}{L} = 0.1$		$\frac{h}{L} = 0.5$	
		$\frac{V}{wL}$	$\frac{F}{wL}$	$\frac{V}{wL}$	$\frac{F}{wL}$
1	0	0.464	−0.186	0.224	−0.447

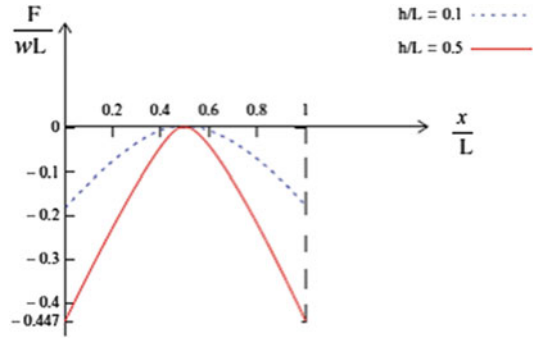

Fig. E6.1c Axial force, F

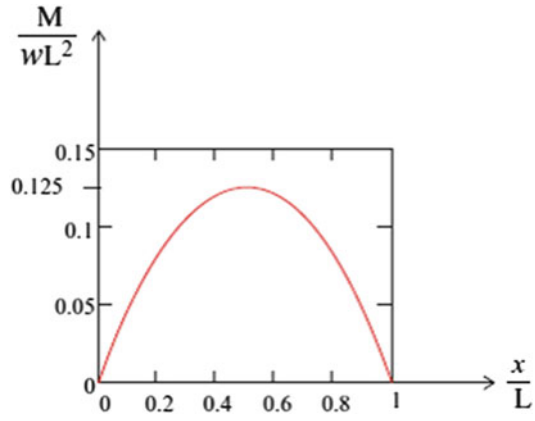

Fig. E6.1d Moment, M

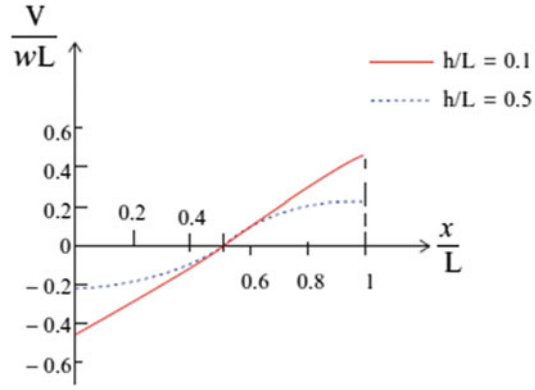

Fig. E6.1e Shear, V

The axial force is compressive and the maximum value occurs at the supports. The maximum shear force also occurs at the supports. The maximum moment occurs at the mid-span. These maximum values are listed below.

$$F_{\max} = \begin{cases} 0.186\,wL & \text{for } \dfrac{h}{L} = 0.1 \\ 0.447\,wL & \text{for } \dfrac{h}{L} = 0.5 \end{cases}$$

$$V_{\max} = \begin{cases} 0.464\,wL & \text{for } \dfrac{h}{L} = 0.1 \\ 0.224\,wL & \text{for } \dfrac{h}{L} = 0.5 \end{cases}$$

$$M_{\max} = 0.125\,wL^2$$

Example 6.2 Shallow vs. Deep Parabolic Curved Members

Given: The parabolic curved beam defined in Fig. E6.2a

Determine: The axial, shear, and moment distributions for (a) $h/L = 0.1$, (b) $h/L = 0.5$.

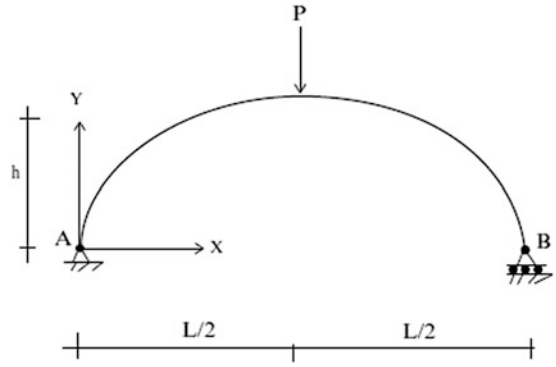

Fig. E6.2a

Solution: Enforcing equilibrium and symmetry leads to the reactions listed in Fig. E6.2b.

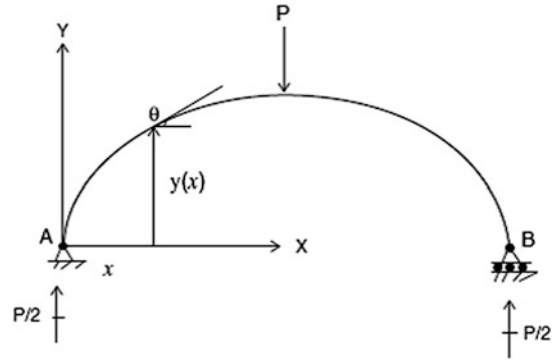

Fig. E6.2b Reactions

Applying (6.4) and (6.5), the internal forces in the local frame are

$$\begin{array}{ll} \text{For} \quad 0 \le x < L/2 & \text{For} \quad L/2 < x \le L \\ F = -\dfrac{P}{2}\sin\theta & F = +\dfrac{P}{2}\sin\theta \\ V = -\dfrac{P}{2}\cos\theta & V = +\dfrac{P}{2}\cos\theta \\ M = \dfrac{P}{2}x & M = +\dfrac{P}{2}(L-x) \end{array}$$

where

$$\cos\theta = \frac{1}{\sqrt{1+\left(4\frac{h}{L}\left(1-2\frac{x}{L}\right)\right)^2}}$$

$$\sin\theta = \frac{4\frac{h}{L}\left(1-2\frac{x}{L}\right)}{\sqrt{1+\left(4\frac{h}{L}\left(1-2\frac{x}{L}\right)\right)^2}}$$

The internal forces are plotted in Figs. E6.1c, E6.1d, and E6.1e and listed in the table which follows for $h/L = 0.1$ and $h/L = 0.5$.

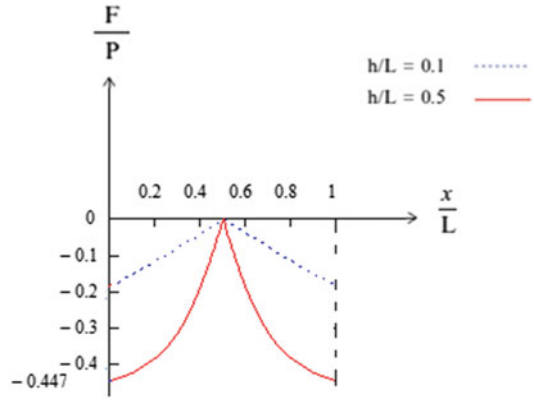

Fig. E6.2c Axial force, F

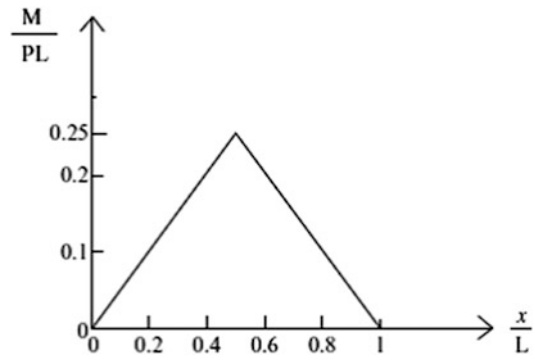

Fig. E6.2d Moment, M

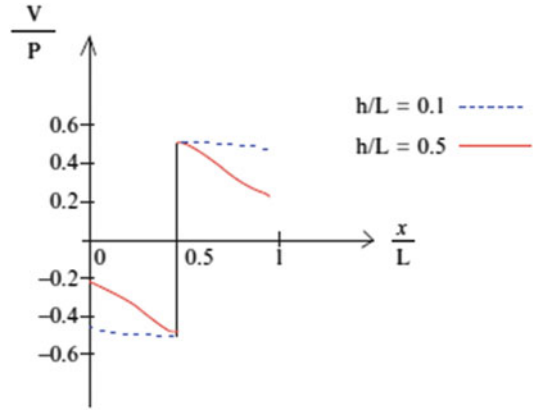

Fig. E6.2e Shear, V

The axial force is compressive and the maximum value occurs at the supports. The maximum shear force and maximum moment occur at the mid-span.

		$\frac{h}{L} = 0.1$		$\frac{h}{L} = 0.5$	
$\frac{x}{L}$	$\frac{M}{PL}$	$\frac{V}{P}$	$\frac{F}{P}$	$\frac{V}{P}$	$\frac{F}{P}$
0	0	−0.464	−0.186	−0.224	−0.447
0.1	0.05	−0.476	−0.152	−0.265	−0.424
0.2	0.1	−0.486	−0.117	−0.32	−0.384
0.3	0.15	−0.494	−0.079	−0.39	−0.312
0.4	0.2	−0.498	−0.04	0.464	−0.186
0.5	0.25	0.5	0	0.5	0
0.6	0.2	0.498	0.04	0.464	0.186
0.7	0.15	0.494	0.079	0.39	0.312
0.8	0.1	0.486	0.177	0.32	0.384
0.9	0.05	0.476	0.152	0.265	0.424
1	0	0.464	0.186	0.244	0.447

6.5 Method of Virtual Forces for Curved Members

Displacements are determined using the form of the method of virtual forces specialized for curved members [1]:

$$d\,\delta P = \int_s \left\{ \frac{F}{AE}\delta F + \frac{V}{GA_s}\delta V + \frac{M}{EI}\delta M \right\} \mathrm{d}s \tag{6.9}$$

where d is the desired displacement, δP, δF, δV, δM denote the virtual force system, and the various terms represent the contribution of axial, shear, and bending deformation. As discussed in Chaps. 3 and 4, the contributions of axial and shear deformation are usually small and only the bending deformation term is retained for slender straight beams and frames composed of slender straight members. *For curved members, we distinguish between "non-shallow" and "shallow" members.*

6.5.1 Non-shallow Slender Curved Members

For non-shallow slender curved members subjected to transverse loading, the contributions of axial and shear deformation are usually small and only the bending deformation term is retained. In this case, we approximate (6.9) with

$$d\,\delta P \approx \int_s \frac{M}{EI}\delta \mathrm{M}\,\mathrm{d}s = \int_x \frac{M\,\delta M}{EI\,\cos\theta}\mathrm{d}x \tag{6.10}$$

6.5.2 Shallow Slender Curved Members

For shallow slender curved members subjected to transverse loading, the axial deformation may be as significant as the bending deformation and therefore *must be retained*. In this case, we use

$$d\,\delta P \approx \int_s \left\{\frac{F}{AE}\delta F + \frac{M}{EI}\delta M\right\}\mathrm{d}s = \int_x \left\{\frac{F}{AE}\delta F + \frac{M}{EI}\delta M\right\}\frac{\mathrm{d}x}{\cos\theta} \tag{6.11}$$

Example 6.3 Deflection of Parabolic Curved Beam—Shallow vs. Deep

Given: The parabolic curved beam defined in Fig. E6.3a. Consider *EI* is constant.

Determine: The horizontal displacement at B for (a) non-shallow beam and (b) shallow beam.

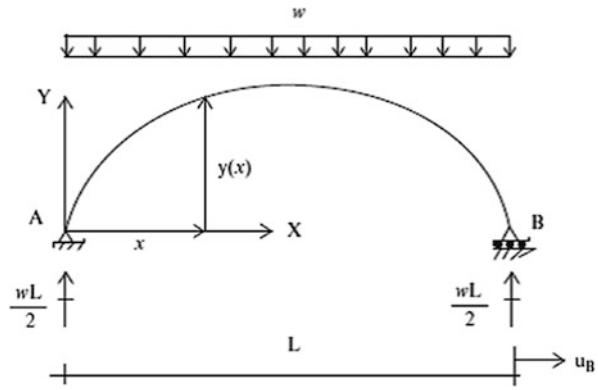

Fig. E6.3a

The internal forces for this loading are

$$\begin{aligned} F_x &= 0 \\ F_y &= -\frac{wL}{2} + wx \end{aligned} \quad \Rightarrow \quad \begin{aligned} F &= \left(-\frac{wL}{2} + wx\right) \sin\theta \\ V &= \left(-\frac{wL}{2} + wx\right) \cos\theta \end{aligned}$$

$$M = \frac{wL}{2}x - \frac{wx^2}{2}$$

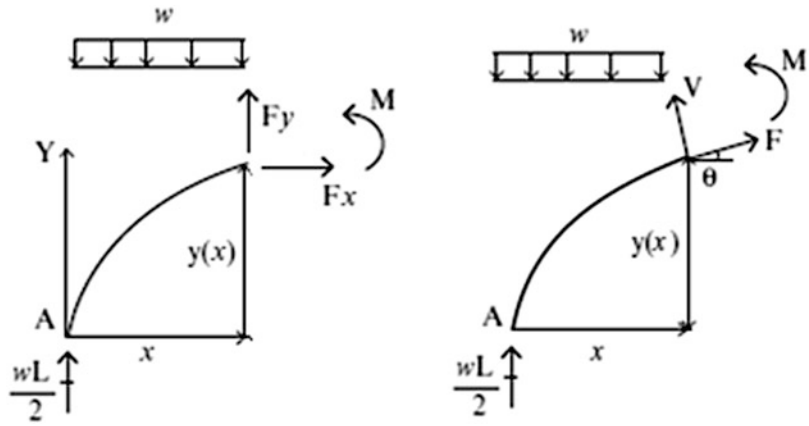

Fig. E6.3b

In order to determine the horizontal displacement at support B, we apply the virtual force system shown in Fig. E6.3c.

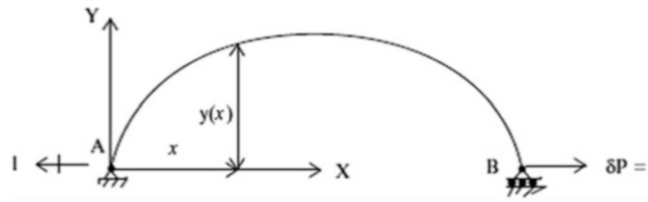

Fig. E6.3c Virtual force system for u_B

The internal virtual forces are

$$\begin{aligned} \delta F_x &= 1 \\ \delta F_y &= 0 \end{aligned} \quad \Rightarrow \quad \begin{aligned} \delta F &= \delta F_y \sin\theta + \delta F_x \cos\theta = \cos\theta \\ \delta V &= \delta F_y \cos\theta - \delta F_x \sin\theta = -\sin\theta \\ \delta M &= y(x) \\ \tan\theta &= \frac{dy}{dx} \end{aligned}$$

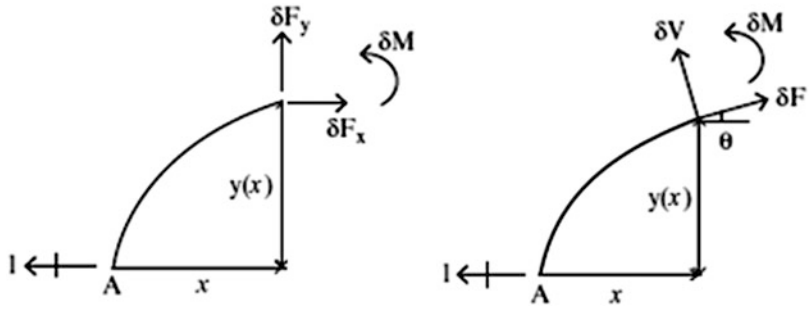

Fig. E6.3d

(a) *Non-shallow curved member*:
We use the approximate form defined by (6.10) for a non-shallow curved member.

$$u_B = \int_0^L \frac{M\,\delta M}{EI\cos\theta}\,dx$$

Substituting for M, δM, and $\cos\theta$, this expression expands to

$$u_B = \int_0^L \left(\frac{wL}{2}x - \frac{wx^2}{2}\right)\left\{4h\left(\frac{x}{L} - \left(\frac{x}{L}\right)^2\right)\right\}\sqrt{1+(\tan\theta)^2}\,\frac{dx}{EI}$$

where

$$\tan\theta = 4\frac{h}{L}\left(1 - 2\frac{x}{L}\right)$$

For EI constant, the solution is expressed as

$$u_B = \frac{wL^4}{EI}(\alpha)$$

where α is a function of h/L. We evaluate α using numerical integration. The result is plotted below.

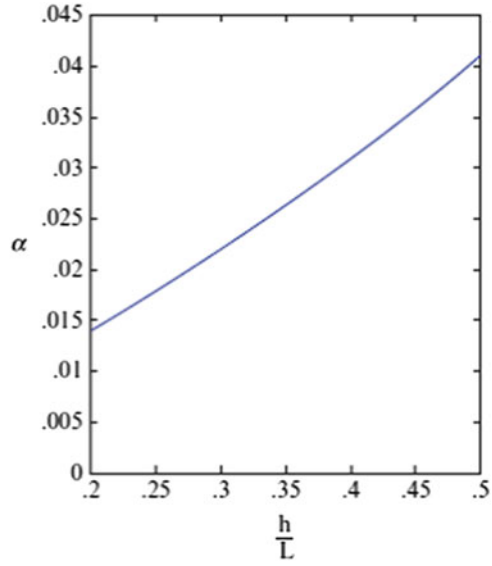

(b) *Shallow curved member*:
When the parabola is shallow ($\cos\theta \approx 1$), we need to include the axial deformation term as well as the bending deformation term. Starting with the form specified for a shallow member, (6.11),

$$u_B = \int_x \left(\frac{F}{AE}\delta F + \frac{M}{EI}\delta M \right) \mathrm{d}x$$

and noting that

$$F \approx \left(-\frac{wL}{2} + wx \right) \frac{\mathrm{d}y}{\mathrm{d}x} = -\frac{2wh}{L^2}(L - 2x)^2$$

$$M = \frac{wL}{2}x - \frac{wx^2}{2}$$

$$\delta F_x = 1 \quad \Rightarrow \quad \delta F = \delta F_x \cos \approx 1$$

$$\delta M = y = 4h\left\{ \frac{x}{L} - \left(\frac{x}{L} \right)^2 \right\}$$

leads to

$$u_B = -\frac{2}{3}\frac{wLh}{AE} + \frac{1}{15}\frac{whL^3}{EI}$$

Note that the axial deformation causes the ends to move together, whereas the bending deformation causes the ends to move apart.

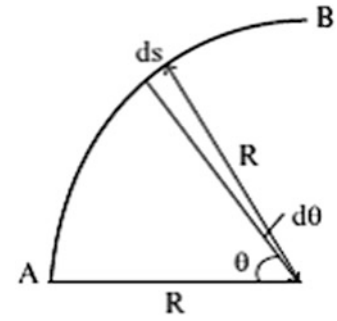

Fig. 6.18 Geometry—circular arch

6.5.3 Circular Curved Member

When the arch geometry is a circular segment, it is more convenient to work with polar coordinates. We consider the segment shown in Fig. 6.18. In this case, R is constant and θ is the independent variable. The differential arc length ds is equal to R dθ.

We assume the member is slender and retain only the bending deformation term. Equation (6.10) takes the following form:

$$d\,\delta P = \int_0^{\theta_B} \frac{M\,\delta M}{EI} R\,\mathrm{d}\theta \tag{6.12}$$

When EI is constant, the equation simplifies to

$$d\,\delta P = \frac{R}{EI}\int_0^{\theta_B} M\,\delta M\,\mathrm{d}\theta \tag{6.13}$$

Example 6.4 Deflection of a Light Pole

Given: The light pole structure defined in Figs. E6.4a, E6.4b, E6.4c, and E6.4d. Consider EI to be constant.

Determine: The horizontal and vertical displacements at C.

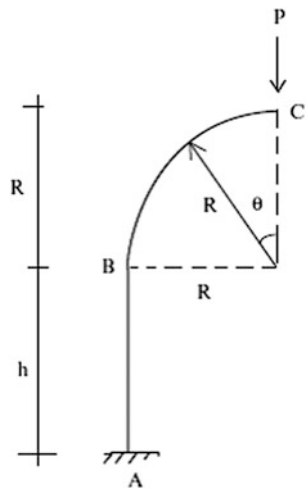

Fig. E6.4a

Solution: Member AB is straight and BC is a circular arc. We take the polar angle from C toward B. The bending moment distribution due to P is

$$\begin{array}{lll} \text{Segment B} - \text{C} & M = -PR\sin\theta & 0 < \theta < \pi/2 \\ \text{Segment A} - \text{B} & M = -PR & 0 < x < h \end{array}$$

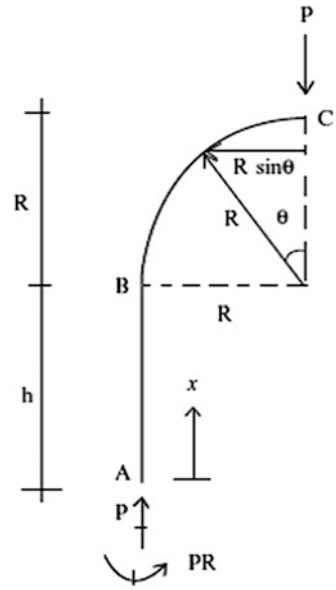

Fig. E6.4b $M(x)$

The vertical displacement at C is determined with the following virtual force system

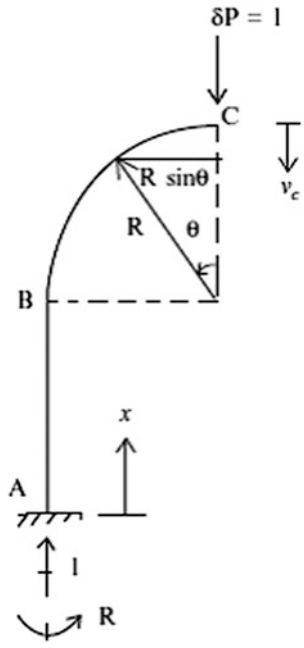

Fig. E6.4c $\delta M(x)$ for v_c

$$\begin{array}{lll} \text{Segment B} - \text{C} & \delta M = -R \sin\theta & 0 < \theta < \pi/2 \\ \text{Segment A} - \text{B} & \delta M = -R & 0 < x < h \end{array}$$

Considering only bending deformation terms, the displacement is given by

$$\begin{aligned} v_c &= v_c|_{AB} + v_c|_{CB} \\ &= \frac{1}{EI}\int_0^h (-PR)(-R)\mathrm{d}x + \frac{1}{EI}\int_0^{\pi/2} (-PR\sin\theta)(-R\sin\theta)R\,\mathrm{d}\theta \\ &= \frac{PR^2h}{EI} + \frac{1}{EI}\int_0^{\pi/2} PR^3(\sin\theta)^2\mathrm{d}\theta \\ &= \frac{PR^2}{EI}\left(h + \frac{\pi}{4}R\right) \end{aligned}$$

Following a similar approach, the virtual force system corresponding to the horizontal displacement at C is evaluated

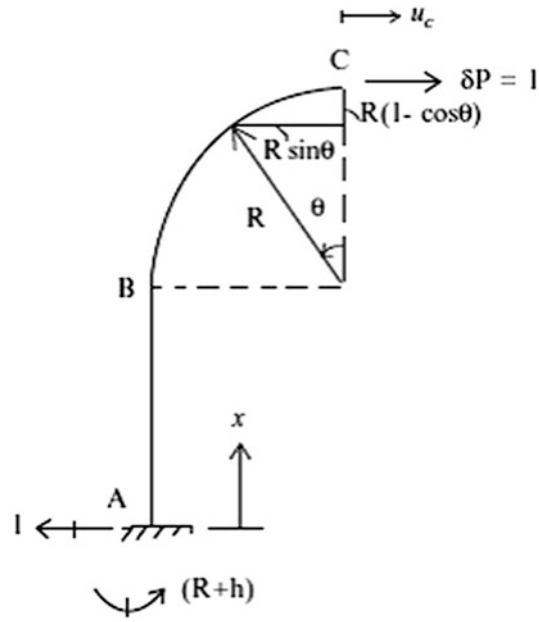

Fig. E6.4d $\delta M(x)$ for u_c

$$\begin{array}{lll} \text{Segment B} - \text{C} & \delta M = -R(1 - \cos\theta) & 0 < \theta < \pi/2 \\ \text{Segment A} - \text{B} & \delta M = -(R + h) + x & 0 < x < h \end{array}$$

Then

$$
\begin{aligned}
u_c &= u_c|_{AB} + u_c|_{BC} \\
&= \frac{1}{EI}\int_0^h (-PR)(-R-h+x)\mathrm{d}x + \frac{1}{EI}\int_0^{\pi/2} (-PR\sin\theta)R(-1+\cos\theta)R\,\mathrm{d}\theta \\
&= \frac{PRh^2}{2EI} + \frac{PR^2h}{EI} + \frac{1}{EI}\int_0^{\pi/2} PR^3(1-\cos\theta)\sin\theta\,\mathrm{d}\theta \\
&= \frac{P}{EI}\left(\frac{R^3}{2} + \frac{h^2R}{2}R^2h\right)
\end{aligned}
$$

6.6 Analysis of Three-Hinged Arches

An arch is a particular type of curved member that is restrained against movement at its ends. Since these restraints produce longitudinal forces which counteract the action of vertical loads, arch structures are generally more efficient than straight members. In this section, we examine three-hinged arches, which are a popular form of arch structure. These structures are statically determinate. A more detailed study of statically indeterminate arches is presented in Chap. 9.

Consider the arch shown in Fig. 6.19. This structure is statically determinate since there is a moment release at C. The overall analysis strategy is as follows:

Step 1: Moment summation about A
Step 2: Moment summation about C for segment CB of the arch

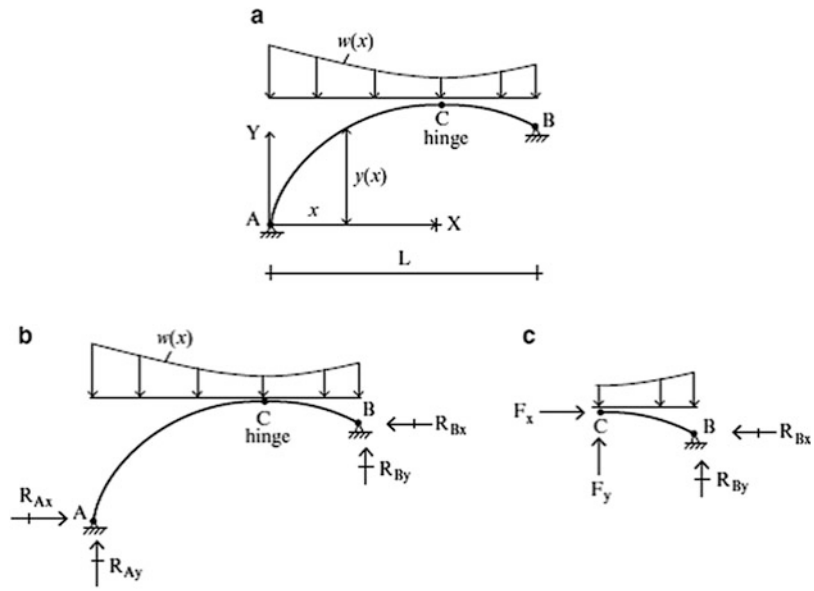

Fig. 6.19 Geometry and reactions—three-hinged arch. (**a**) Geometry. (**b**) Reactions. (**c**) Right segment

These steps result in two equations relating R_{Bx} and R_{By}, which can be solved.

Step 3: X force summation $\rightarrow R_{Ax}$
Step 4: Y force summation $\rightarrow R_{Ay}$

Once the reactions are known, one can work in from either end and determine the internal forces and moment using the equations derived in the previous section. The following examples illustrate the approach.

Example 6.5 Three-Hinged Parabolic Arch

Given: The three-hinged arch shown in Fig. E6.5a.

Determine: The reactions. Assume $L_1 = 30$ m, $w = 15$ kN/m.

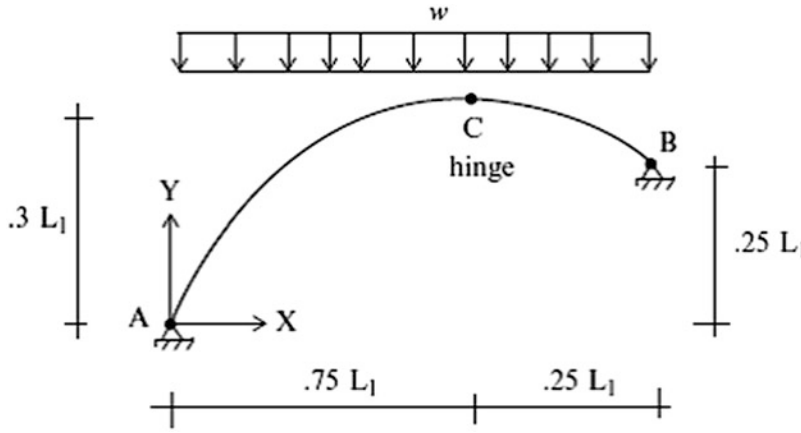

Fig. E6.5a

Solution: Summing moments about A and C leads to (Figs. E6.5b and E6.5c)

$$\sum M_{\text{at A}} = 0 \quad -w\frac{(L_1)^2}{2} + B_x(0.25L_1) + B_y(L_1) = 0$$

$$\sum M_{\text{at C}} = 0 \quad -w\frac{(0.25L_1)^2}{2} - B_x(0.05L_1) + B_y(0.25L_1) = 0$$

The solution of the above equations leads to

$$B_x = \frac{5}{6}wL_1 = 375\,\text{kN}\leftarrow$$

$$B_y = \frac{7}{24}wL_1 = 131.25\,\text{kN}\uparrow$$

Lastly, the reactions at A are determined using force equilibrium:

$$\sum F_y = 0 \quad A_y = -B_y + wL_1 = \frac{17}{24}wL_1 = 318.75\,\text{kN}\uparrow$$

$$\sum F_x = 0 \quad A_x = -B_x = 375\,\text{kN}\rightarrow$$

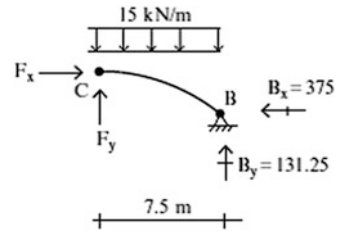

Fig. E6.5b

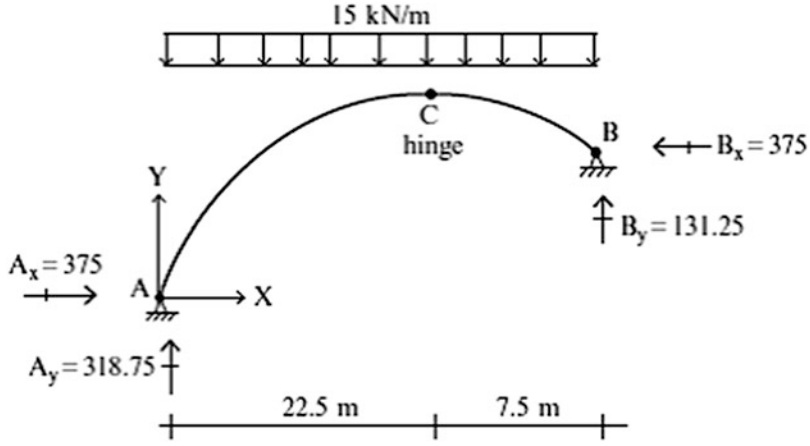

Fig. E6.5c

Example 6.6 Three-Hinged Parabolic Arch—Uniform Vertical Loading

Given: The parabolic arch shown in Fig. E6.6a.

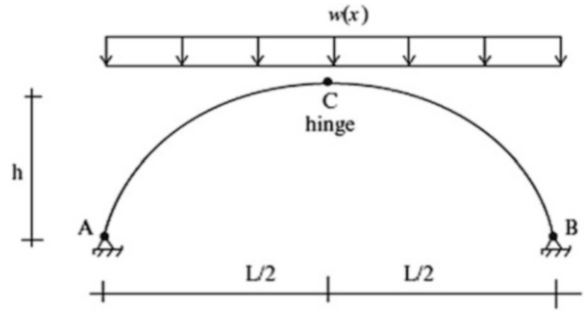

Fig. E6.6a

Determine: The internal forces and the vertical displacement at C (v_c).

Solution: The loading and arch geometry are symmetrical with respect to mid-span. It follows that the vertical reactions are equal to $wL/2$. Setting the moment at C equal to zero, we obtain an expression for R_{Bx} (Fig. E6.6b).

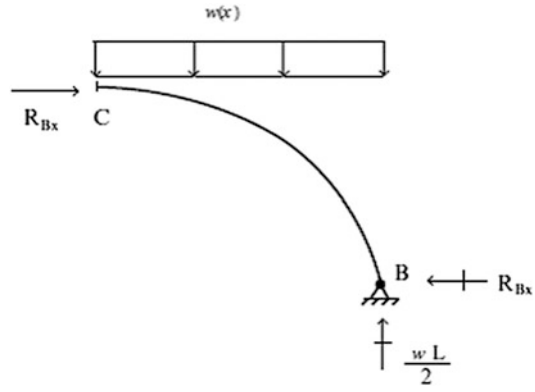

Fig. E6.6b

$$\sum M_c^{+\circlearrowright} = 0$$

$$\frac{w}{2}\left(\frac{L}{2}\right)^2 + hR_{\mathrm{Bx}} = \frac{wL}{2}\frac{L}{2} \rightarrow \quad R_{\mathrm{Bx}} = \frac{wL^2}{8h} \leftarrow$$

Then, summing X forces,

$$\sum F_x = 0$$

$$R_{\mathrm{A}x} = \frac{wL^2}{8h} \rightarrow$$

The results are listed below (Figs. E6.6b and E6.6c).

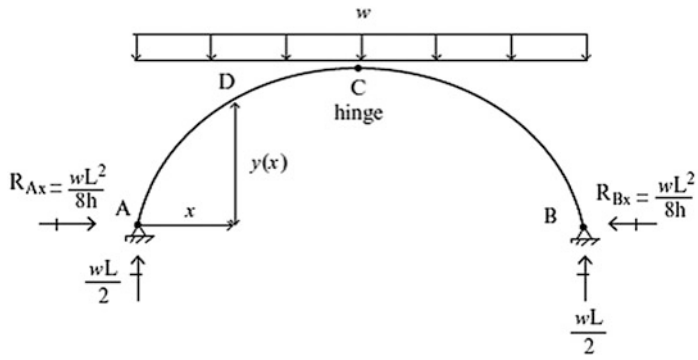

Fig. E6.6c

Cutting the member at D, isolating the segment AD, and applying the equilibrium conditions lead to:

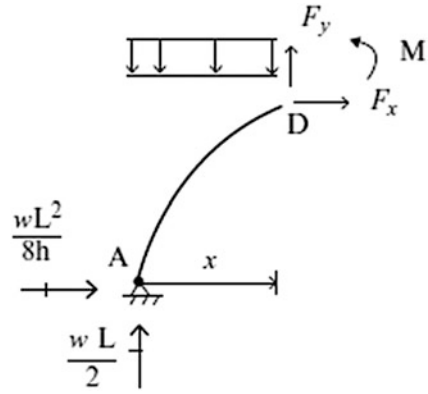

Fig. E6.6d

$$F_x = -\frac{wL^2}{8h}$$
$$F_y = wx - \frac{wL}{2}$$
$$M = \frac{wL}{2}x - \frac{wL^2}{8h}y - \frac{wx^2}{2}$$

Substituting for y, the expression for M reduces to

$$M = \frac{wL}{2}x - \frac{wL^2}{8h}\left\{4h\left[\frac{x}{L} - \left(\frac{x}{L}\right)^2\right]\right\} - \frac{wx^2}{2} = 0$$

It follows that there is no bending moment in a three-hinged parabolic arch subjected to uniform loading per horizontal projection.

We could have deduced this result from the theory of cables presented in Chap. 5. We showed there that a cable subjected to a uniform vertical loading per horizontal projection adopts a parabolic shape. A cable, by definition, has no moment. Therefore, if one views a parabolic arch as an inverted cable, it follows that the moment in the arch will be zero. *This result applies only for uniform vertical loading; there will be bending for other types of loading applied to a parabolic arch.*

The axial force and transverse shear are determined with (6.2).

$$F = F_x \cos\theta + F_y \sin\theta = -\frac{wL^2}{8h}\cos\theta + \left(wx - \frac{wL}{2}\right)\sin\theta$$
$$V = -F_x \sin\theta + F_y \cos\theta = -\frac{wL^2}{8h}\sin\theta + \left(wx - \frac{wL}{2}\right)\cos\theta$$

where

$$\tan\theta = \frac{4h}{L}\left(1 - 2\frac{x}{L}\right)$$
$$\cos\theta = \frac{1}{\sqrt{1 + \tan\theta^2}}$$
$$\sin\theta = \frac{\tan\theta}{\sqrt{1 + \tan\theta^2}}$$

Expanding theexpression for V and substituting for tan θ, one finds

$$V = \left[\tan\theta\frac{wL^2}{8h} + wx - \frac{wL}{2}\right]\cos\theta \equiv 0$$

The shear must be zero since the moment is zero. Only axial force exists for this loading.

The axial force distribution is plotted below. The maximum value is also tabulated as a function of h/L.

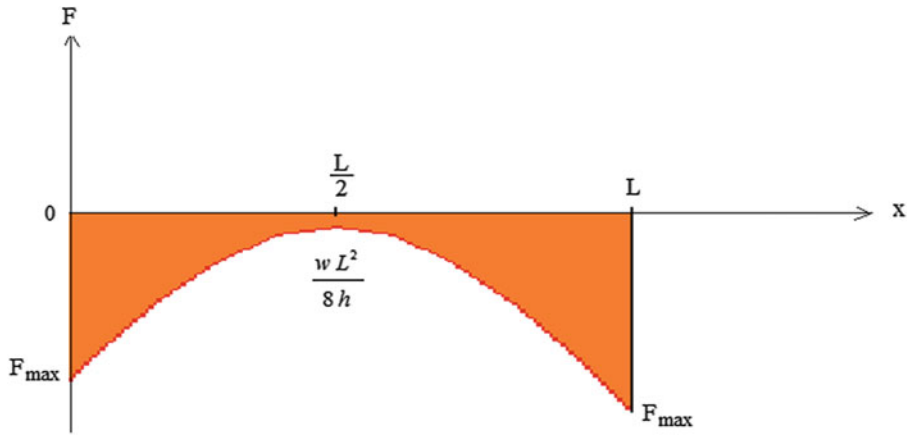

h/L	$F_{\max}$
0.1	$-1.35wL$
0.2	$-0.8wL$
0.3	$-0.65wL$
0.4	$-0.59wL$
0.5	$-0.56wL$

The solution, $M = V = 0$, is valid for a uniformly loaded three-hinged parabolic arch, i.e., it applies for both *deep and shallow* arches.

If we use the approximate form of the method of virtual forces specialized for a "deep" arch,

$$v_c = \int_S \frac{M\,\delta M}{EI}\mathrm{d}s$$

it follows that the arch does not displace due to bending deformation. However, there will be displacement due to the axial deformation. We need to start with the exact expression,

$$v_c = \int_S \left(\frac{M\,\delta M}{EI} + \frac{F\,\delta F}{EA}\right)\mathrm{d}s$$

and then set $M = 0$

$$v_c \cong \int_S \frac{F\,\delta F}{EA}\mathrm{d}s$$

Suppose the vertical displacement at mid-span is desired. The virtual force system for $\delta P = 1$ is

$$\begin{aligned}\delta F_x &= -\frac{L}{4h}\\ \delta F_y &= -\frac{1}{2}\end{aligned} \quad \Rightarrow \quad \delta F = \left(-\frac{L}{4h}\right)\cos\theta + \left(-\frac{1}{2}\right)\sin\theta$$

Substituting for the forces and assuming AE is constant result in the following integral

$$v_c = \frac{1}{AE}\int_0^L \left\{\left(-\frac{wL^2}{8h}\right) + \left(-\frac{wL}{2} + wx\right)\tan\theta\right\}\left(-\frac{L}{4h} - \frac{1}{2}\tan\theta\right)\cos\theta\,dx$$

We express the solution as

$$v_c = \frac{wL^2}{AE}\{\alpha\}$$

where α is a function of h/L. The following plot shows the variation of α. Note that v_c approaches 0 for a deep arch.

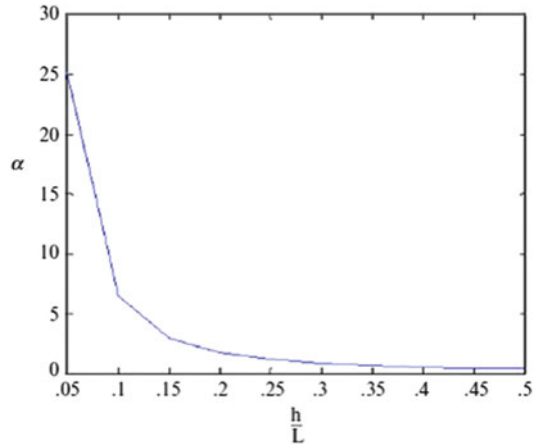

Example 6.7 Three-Hinged Parabolic Arch—Concentrated Load Applied at Mid-Span

Given: The parabolic arch defined in Fig. E6.7a

Determine: The internal forces and vertical displacement at C (v_c).

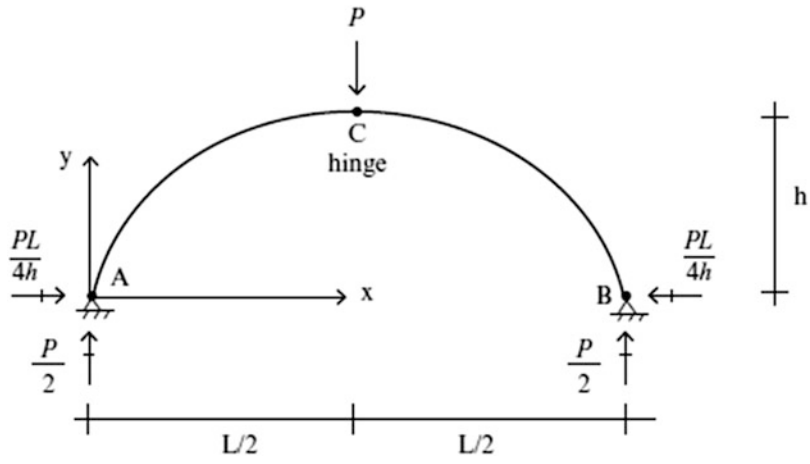

Fig. E6.7a

Solution: Enforcing equilibrium leads to the following expressions for the internal forces (Fig. E6.7b):

Segment AC $0 \leq x < L/2$

$$F_x = -\frac{PL}{4h}$$
$$F_y = -\frac{P}{2}$$
$$M = \frac{P}{2}x - \frac{PL}{4h}y$$

Segment CB $L/2 < x \leq L$

$$F_x = -\frac{PL}{4h}$$
$$F_y = \frac{P}{2}$$
$$M = -\frac{P}{2}x - \frac{PL}{4h}y + \frac{PL}{2}$$

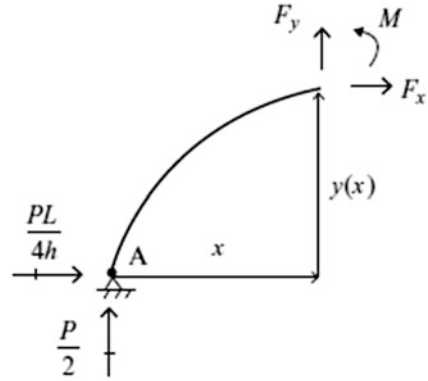

Fig. E6.7b

The corresponding transformed internal forces are

Segment AC $0 \leq x < L/2$

$$F = -\frac{P}{2}\sin\theta - \frac{PL}{4h}\cos\theta$$
$$V = -\frac{P}{2}\cos\theta + \frac{PL}{4h}\sin\theta$$
$$M = \frac{P}{2}x - PL\left[\frac{x}{L} - \left(\frac{x}{L}\right)^2\right] = PL\left(-\frac{x}{2L} + \frac{x^2}{L^2}\right)$$

Segment CB $L/2 < x \leq L$

$$F = \frac{P}{2}\sin\theta - \frac{PL}{4h}\cos\theta$$

$$V = \frac{P}{2}\cos\theta + \frac{PL}{4h}\sin\theta$$

$$M = PL\left(-\frac{3x}{2L} + \frac{x^2}{L^2} + \frac{1}{2}\right)$$

The values of F, V, and M are listed below.

		$h/L = 0.5$		$h/L = 0.1$	
X/L	M/PL	F/P	V/P	F/P	V/P
0	0	−0.67	0.22	−2.51	0.46
0.1	−0.04	−0.69	0.16	−2.53	0.3
0.2	−0.06	−0.7	0.06	−2.55	0.1
0.3	−0.06	−0.7	−0.08	−2.55	−0.1
0.4	−0.04	−0.65	0.28	−2.53	−0.3
0.5	0	−0.5	∓0.5	−2.5	∓0.5
0.6	−0.04	−0.65	0.28	−2.53	0.3
0.7	−0.06	−0.7	0.08	−2.55	0.1
0.8	−0.06	−0.7	0.06	−2.55	−0.1
0.9	−0.04	−0.69	−0.16	−2.53	−0.3
1	0	−0.67	−0.22	−2.51	−0.46

The maximum moment occurs at the location where $dM/dx = 0$. Note that $M_{max} = +PL/4$ for a straight member.

$$\frac{dM}{dx} = 0 \quad \Rightarrow \quad x\big|_{M_{max}} = \frac{L}{4} \Rightarrow \quad M_{max} = -\frac{PL}{16}$$

The distribution of F, V, and M is plotted below. The reversal in sense of M is due to the influence of the horizontal thrust force on the bending moment (Figs. E6.7c, E6.7d, and E6.7e).

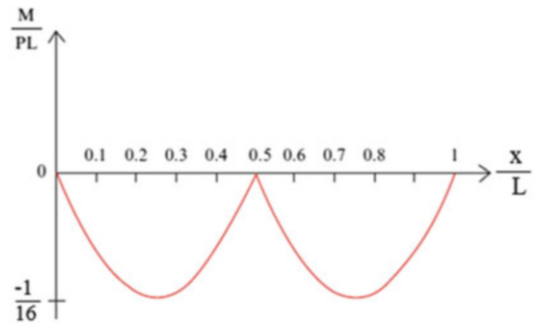

Fig. E6.7c

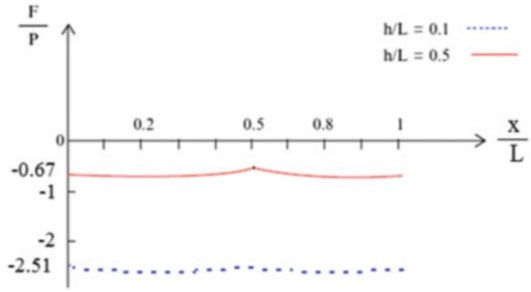

Fig. E6.7d

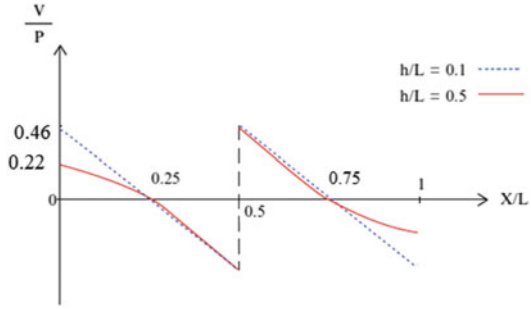

Fig. E6.7e

The virtual forces for the computation of v_c are (Fig. E6.7f)

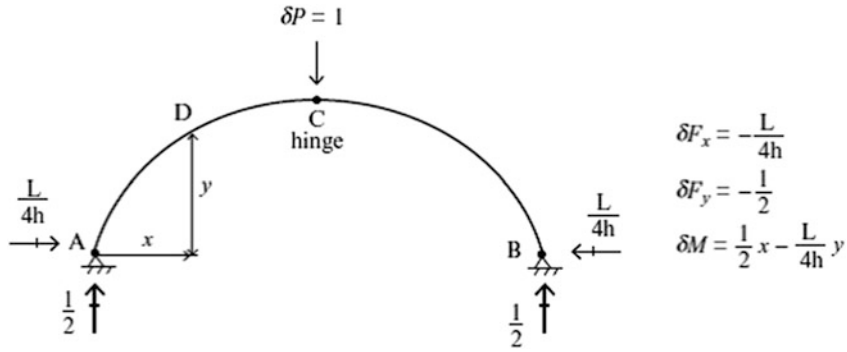

Fig. E6.7f

We consider only bending deformation. The displacement at C is given by

$$v_c = 2\int_0^{L/2} \frac{P}{2}\left(x - \frac{L}{2h}y\right)\frac{1}{2}\left(x - \frac{L}{2h}y\right)\frac{dx}{EI\cos\theta}$$

When I is a function of x, we use either symbolic or numerical integration. However, when I is taken as $I_0/\cos\theta$, the integral simplifies and one can obtain an analytical solution. The analytical solution corresponding to this assumption is

$$v_c = \frac{PL^3}{EI_0}\left(\frac{1}{30}\right)$$

Example 6.8 Three-Hinged Parabolic Arch with Horizontal and Vertical Loads

Given: The parabolic arch and loading defined in Fig. E6.8a.

Determine: (a) Determine the analytical expressions for the axial force, shear force, and bending moment. (b) Using computer software, determine the vertical and horizontal displacements at C due to the loading. Take $E = 29{,}000$ ksi, $I = 5000$ in.^{4}, and $A = 500$ in.^{2} Discretize the arch using segments of length $\Delta x = 1$ ft. Also determine profiles for displacement, moment, and axial force.

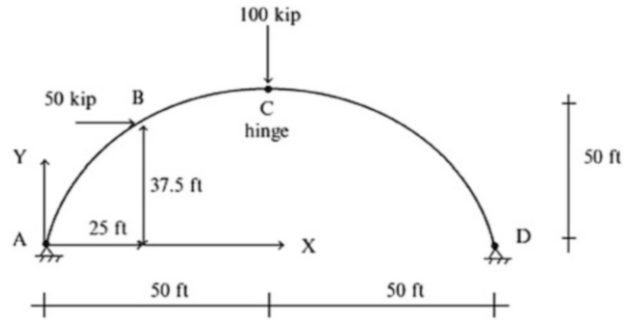

Fig. E6.8a

Solution: (a) The reactions are listed on Fig. E6.8b.

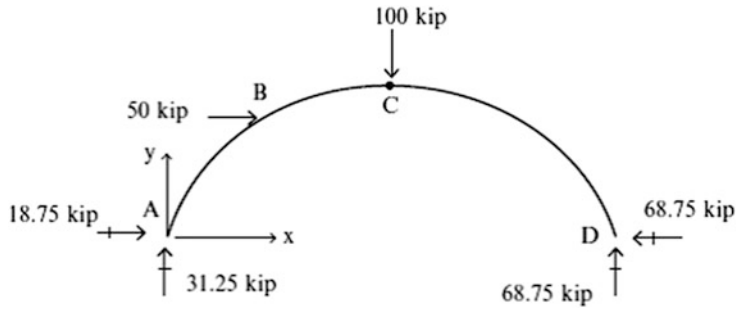

Fig. E6.8b

Noting that $y = 2(x - x^2/100)$ and isolating different segments along the centroidal axis lead to the following expressions for moment (M), axial force (F), and shear (V).
Segment AB $0 \leq x < 25$

$$\begin{aligned} F_x &= -18.75 \\ F_y &= -31.25 \\ M &= 31.25x - 18.75y \end{aligned} \quad \Rightarrow \quad \begin{aligned} F &= -18.75\cos\theta - 31.25\sin\theta \\ V &= -18.75\sin\theta - 31.25\cos\theta \\ M &= 31.25x - 18.75y \end{aligned}$$

Segment BC $25 < x < 50$

$$\begin{aligned} F_x &= -68.75 \\ F_y &= -31.25 \\ M &= 31.25x - 18.75y - 50(y - 37.5) \end{aligned} \quad \Rightarrow \quad \begin{aligned} F &= -68.75\cos\theta - 31.25\sin\theta \\ V &= -68.75\sin\theta - 31.25\cos\theta \\ M &= 31.25x - 18.75y - 50(y - 37.5) \end{aligned}$$

Segment CD $50 < x \leq 100$

$$\begin{aligned} F_x &= -68.75 \\ F_y &= 68.75 \\ M &= 68.75(100 - x) - 68.75y \end{aligned} \quad \Rightarrow \quad \begin{aligned} F &= -68.75\cos\theta + 68.75\sin\theta \\ V &= 68.75\sin\theta + 68.75\cos\theta \\ M &= 68.75(100 - x) - 68.75 \end{aligned}$$

(b) The computer generated moment, axial force, and deflection profiles are listed below (Figs. E6.8c, E6.8d, and E6.8e). Hand computation is not feasible for this task.

Fig. E6.8c Moment, M

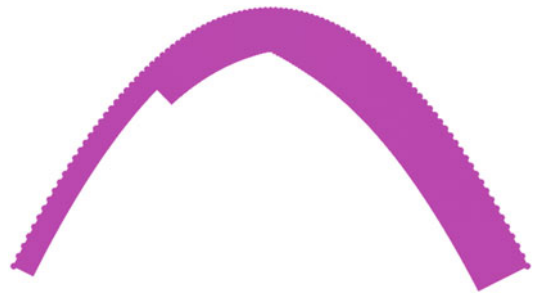

Fig. E6.8d Axial, F

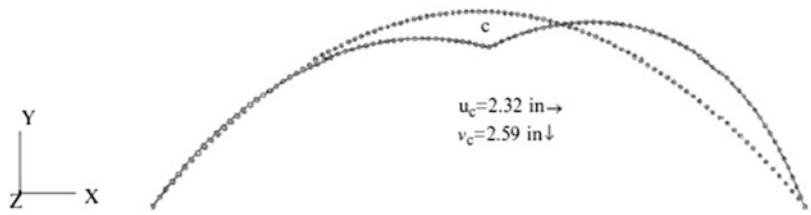

Fig. E6.8e Deflection profile

Example 6.9 Optimal Shape for a Statically Determinate Arch

Given: The loading defined in Fig. E6.9a and support locations A and B. Assume H is a variable.

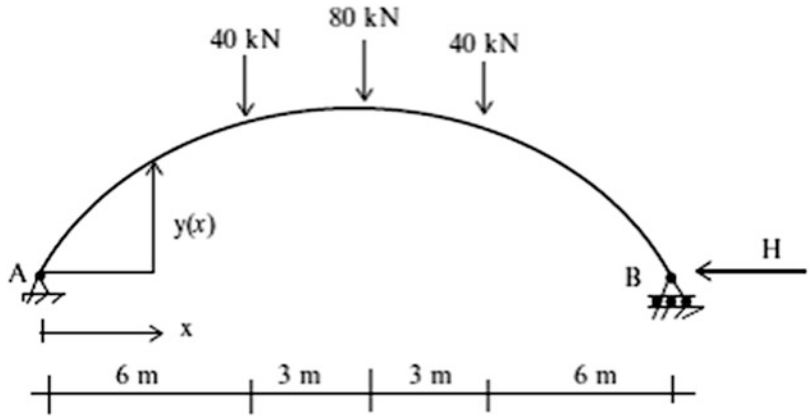

Fig. E6.9a

Determine: The optimal shape of the arch passing through A and B. Consider H to vary from 80 to 200 kN. Note that the optimum shape corresponds to zero bending moment.

Solution: We first generate the bending moment distribution in a simply supported beam spanning between A and B (Fig. E6.9b).

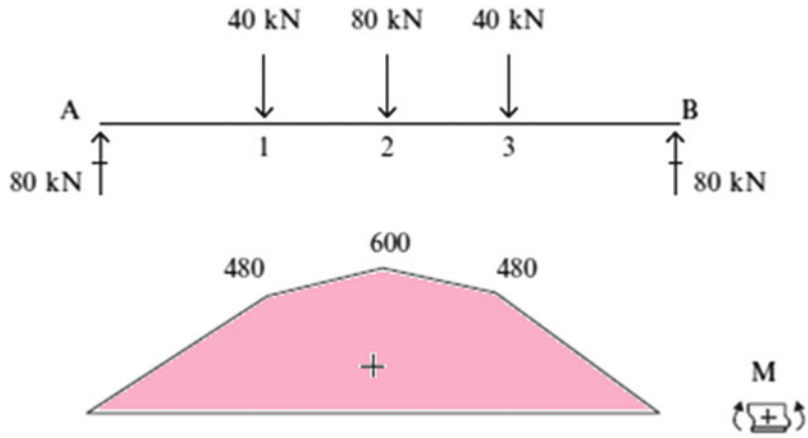

Fig. E6.9b

Requiring the bending moment to vanish at points 1, 2, 3 leads to the following y coordinates of points 1, 2, and 3:

$$y_1 = \frac{480}{H} \quad y_2 = \frac{600}{H} \quad y_3 = \frac{480}{H}$$

This piecewise solution is the general solution for the optimal shape (Fig. E6.9c). One specifies H and then determines the coordinates. The value of H selected depends on the capacity of the supports to resist lateral loading.

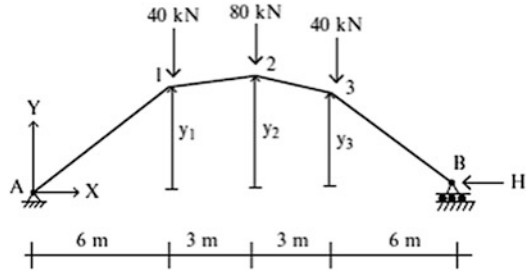

Fig. E6.9c Optimal shape

Configurations corresponding to various values of H are listed below. Note that as H increases, the shape becomes shallower.

H (kN)	y_1 (m)	y_2 (m)	y_3 (m)
80	6	7.5	6
120	4	5	4
160	2	3.75	3
200	1.4	3	2.4

6.7 Summary

6.7.1 Objectives

- To develop the equilibrium equations for planar curved members and illustrate their application to parabolic and circular arches.
- To introduce and apply the Principle of Virtual Forces for planar curved members.
- To describe the analysis process for three-hinged arches.
- To illustrate the behavior of statically determinate parabolic arches subjected to vertical and lateral loading.

6.7.2 Key Factors and Concepts

- Depending upon the loading distribution, the geometry of the member, and the support conditions, a curved member may support transverse loading mainly by axial action. This feature makes curved members very attractive for long span structures.
- Curved members are classified as either shallow or non-shallow, depending upon the ratio of height to span length. For shallow members, bending and axial actions are coupled. In the limit, a shallow curved member reduces to a beam.
- When applying the principle of virtual forces to compute displacements of a slender non-shallow (deep) curved member, the contributions due to axial and shear deformation are usually negligible compared to the contribution from bending deformation.

- In general, three-hinged arches carry load through both bending and axial action. However, when the arch shape is parabolic and the vertical loading is uniform, there is no bending moment in the three-hinged arch.
- Two-hinged curved members are statically indeterminate. A general theory for these structures is presented in Chap. 9. One can show that, based on this theory, a moment free state can be obtained for an arbitrary loading by adjusting the shape of the curved member. In this case, two-hinged curved members behave similar to cables.

6.8 Problems

Problem 6.1 Consider the parabolic member shown below. Find the reactions and member forces (F, V, and M).

(a) Assume $w = 1.2$ kip/ft, $h = 24$ ft, $L = 120$ ft
(b) Assume $w = 18$ kN/m, $h = 7$ m, $L = 36$ m

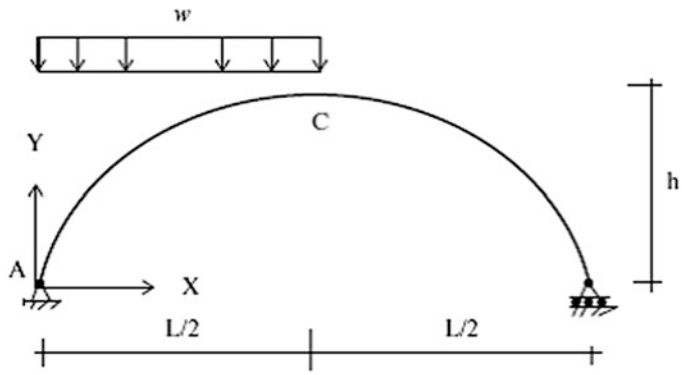

Problem 6.2 Consider the parabolic member shown below. Find the reactions and member forces at $x = 20$ and 80 ft.

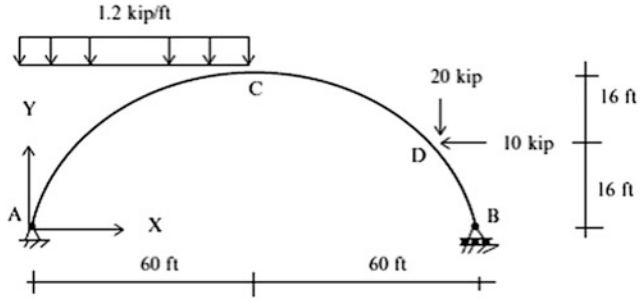

Problem 6.3 Consider the parabolic member shown below. Find the reactions and member forces (F, V, and M).

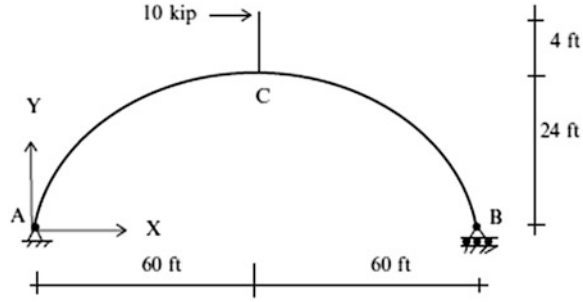

Problem 6.4 Determine the reactions, the axial and shear forces, and the moments at $x = 30$ ft for the three-hinged parabolic arch shown below.

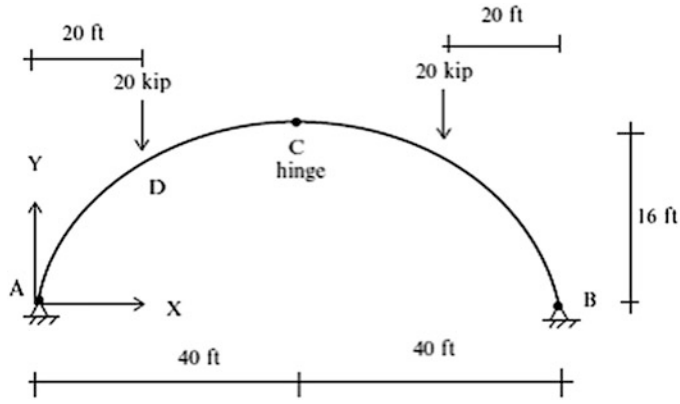

Problem 6.5 Consider the three-hinged circular arch shown below

(a) Find the reactions.
(b) Determine the axial and shear forces and the moments at $x = 20$ ft and $x = 40$ ft.

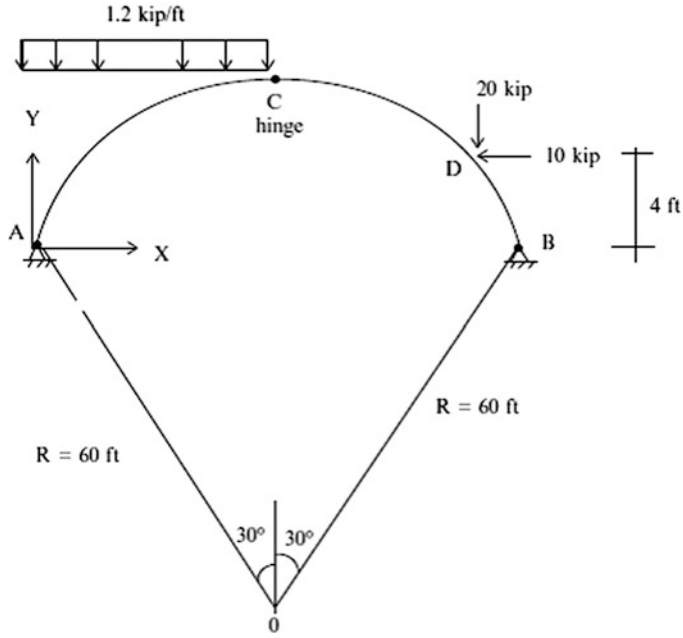

Problem 6.6 Consider the three-hinged parabolic arches shown below. Determine analytical expression for the axial force, shear force, and bending moment. Using computer software, determine displacement profiles. Take $h = 9$ m, $L = 30$ m, $P = 450$ kN, $w = 30$ kN/m, $E = 200$ GPa, $I = 160$ (10^6)mm^4, and $A = 25{,}800$ mm^2

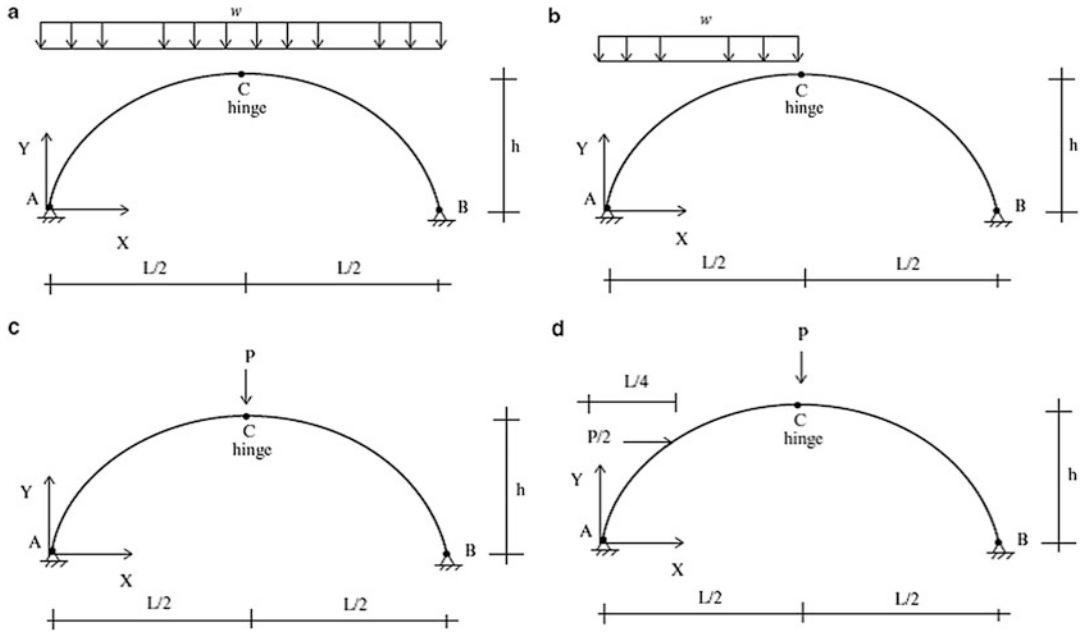

Problem 6.7 Consider the simply supported curved member shown below. Assume the shape is defined by an arbitrary function, $y = y(x)$. Suppose the member experiences a uniform temperature increase, ΔT, over its entire length. Determine the horizontal displacement of B.

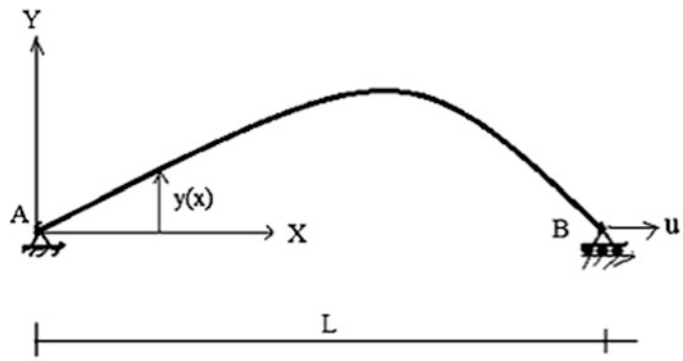

Problem 6.8 Consider the parabolic member shown below. Determine the horizontal displacement at B.

(a) Assume $w = 1.2$ kip/ft, $h = 24$ ft, $L = 120$ ft, $E = 29{,}000$ ksi
(b) Assume $w = 18$ kN/m, $h = 7$ m, $L = 36$ m, $E = 200$ GPa

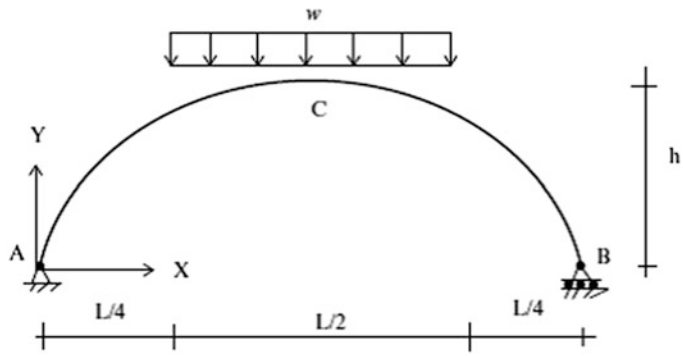

Problem 6.9 Consider the parabolic member shown below. Determine the vertical displacement at C. Take $I = 400$ in.^{4}, $A = 40$ in.^{2}, $E = 29{,}000$ kip/in.^{2}

(a) $h = 10$ ft
(b) $h = 30$ ft

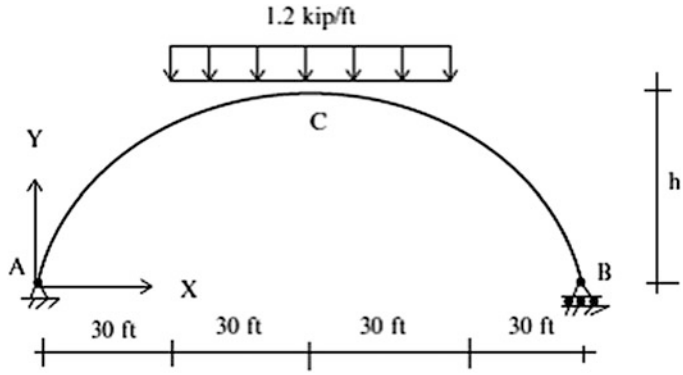

Problem 6.10

(a) Determine analytical expressions for the member forces for the circular curved member shown below. Take $R = 40$ ft, $P = 10$ kip, and $\theta = 30°$.
(b) Repeat part (a) using a computer software package. Discretize the arc length into 3° segments. Assume the following values for the member properties: $E = 29{,}000$ ksi, $I = 400$ in.^{4}, and $A = 40$ in.^{2} Compare the analytical and computer generated values for moment and axial force.

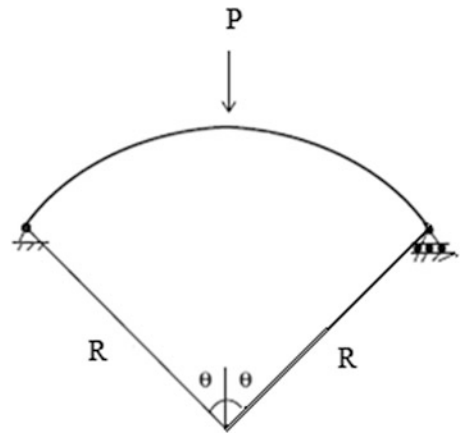

Problem 6.11 Consider the three-hinged arch shown below. Discuss how the arch behaves when:

(a) There is a uniform temperature increase.
(b) The support at B settles.

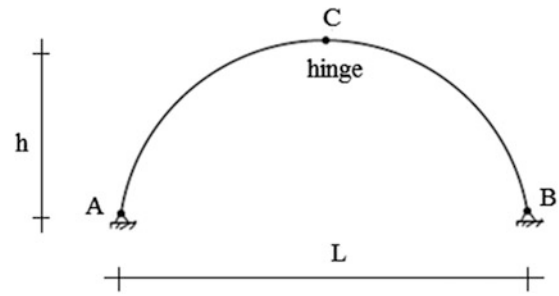

Problem 6.12 Consider the semicircular three-hinged arch shown below. Determine the vertical and horizontal displacements at C due to the loading.

(a) Assume $E = 29{,}000$ ksi, $I = 400$ in.^{4}, $A = 40$ in.^{2}, $R = 50$ ft, and $w = 2$ kip/ft
(b) Assume $E = 200$ GPa, $I = 160(10^6)$ mm^4, $A = 25{,}800$ mm^2, $R = 15$ m, and $w = 30$ kN/m

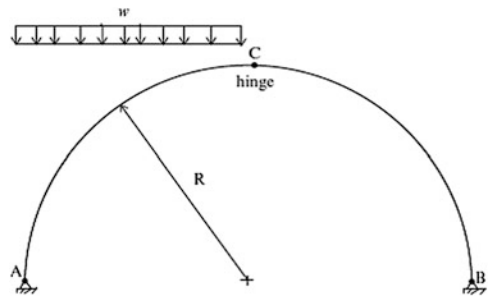

Problem 6.13 Consider the parabolic three-hinged arch shown below. Using computer software, determine the vertical and horizontal displacements at C due to the loading. Discretize the arch using segments of length $\Delta x = L/10$, $L/20$, and $L/40$. Compare the convergence rate for these segment sizes.

(a) Take $E = 29{,}000$ ksi, $I = 400$ in.^{4}, $A = 40$ in.^{2}, $L = 120$ ft, $h = 60$ ft, and $w = 2$ kip/ft
(b) Take $E = 200$ GPa, $I = 160(10^6)$ mm^4, $A = 2500$ mm^2, $L = 36$ m, $h = 18$ m, and $w = 30$ kN/m

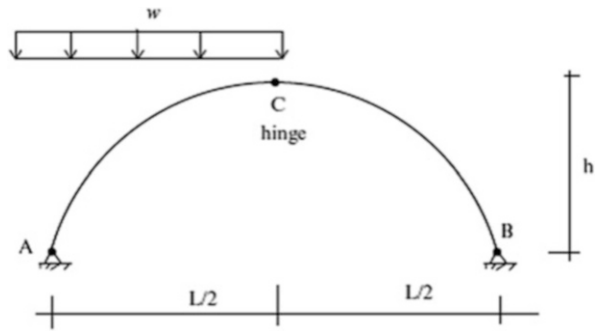

Problem 6.14 Consider the semicircular curved member shown below. Member CD is rigidly attached to the curved member at C. Determine an expression for the horizontal displacement at D due to P.

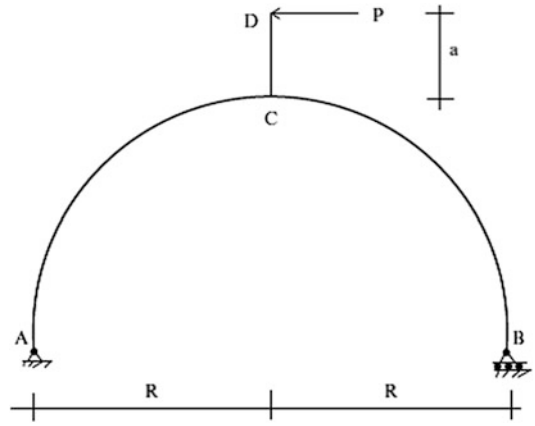

Problem 6.15

(a) Determine analytical solutions for the axial, shear, and moment distribution for the three-hinged semicircular arch shown. Consider the loading to be due to self-weight w. Take $w = 0.6$ kip/ft and $R = 40$ ft.

(b) Apply computer software using the following discretization: $\Delta\theta = 9°, 4.5°, 2.25°$. Compare the convergence rate of the solution. Take $E = 29{,}000$ ksi, $I = 400$ in.^{4}, and $A = 40$ in.^{2}

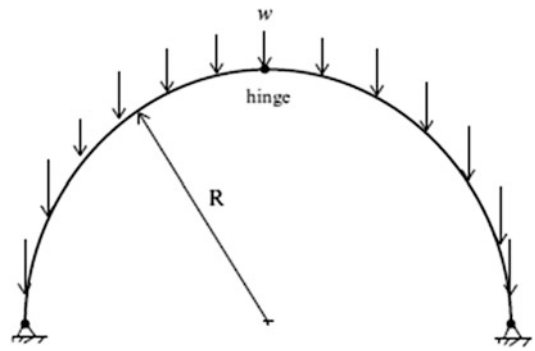

Problem 6.16 Determine the member forces for the three-hinged circular arch shown. Use computer software.

(a) Take $E = 29{,}000$ ksi, $R = 40$ ft, $P = 4$ kip, $I = 400$ in.^{4}, and $A = 40$ in.^{2}

(b) Take $E = 200$ GPa, $R = 12$ m, $P = 18$ kN, $I = 160(10^6)$ mm^4, and $A = 25{,}800$ mm^2

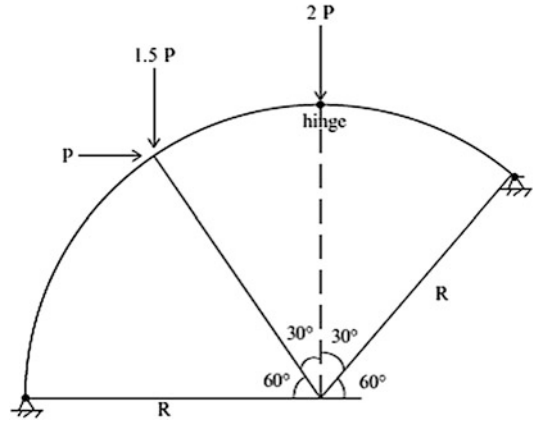

Problem 6.17 Determine the optimal shape of the arch passing through A and B for given value of H. Note that optimum shape corresponds to zero moment. Assume $L = 120$ ft and $P = 25$ kip.

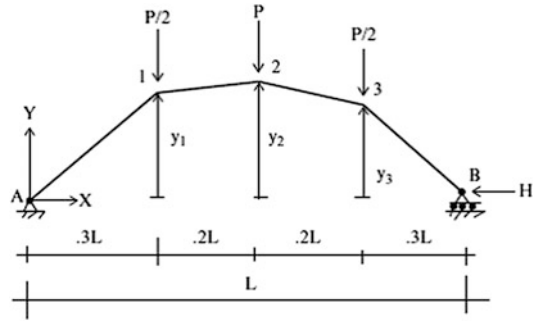

Problem 6.18 Determine the optimal shape of the arch for a given value of H. Assume $L = 30$ m and $w_0 = 15$ kN/m.

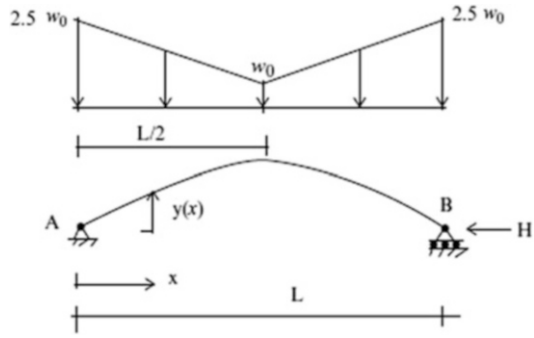

Problem 6.19 Consider the three-hinged arch shown below. Determine the reactions and the internal forces.

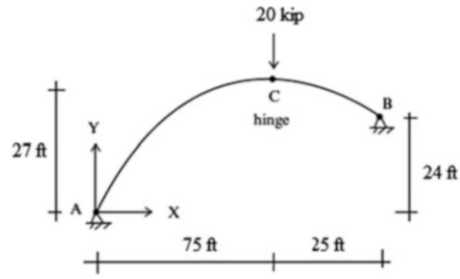

Reference

1. Tauchert TR. Energy principles in structural mechanics. New York: McGraw-Hill; 1974.